

Activation Learning by Local Competitions

Hongchao Zhou

Abstract

The backpropagation that drives the success of deep learning is most likely different from the learning mechanism of the brain. In this paper, we develop a biology-inspired learning rule that discovers features by local competitions among neurons, following the idea of Hebb’s famous proposal. It is demonstrated that the unsupervised features learned by this local learning rule can serve as a pre-training model to improve the performance of some supervised learning tasks. More importantly, this local learning rule enables us to build a new learning paradigm very different from the backpropagation, named activation learning, where the output activation of the neural network roughly measures how probable the input patterns are. The activation learning is capable of learning plentiful local features from few shots of input patterns, and demonstrates significantly better performances than the backpropagation algorithm when the number of training samples is relatively small. This learning paradigm unifies unsupervised learning, supervised learning and generative models, and is also more secure against adversarial attack, paving a road to some possibilities of creating general-task neural networks.

I. INTRODUCTION

The backpropagation algorithm [1] has driven recent success of machine learning, in tasks of speech and image recognition [2], [3], language processing [4], image and music creation [5], as well as playing human games like Go [6], [7] and poker [8]. Many scientists believe that the backpropagation algorithm, although a very powerful tool to train neural networks towards a target function, is different from the rules governing human learning [9]–[12]. The brain seems to learn in a predominantly unsupervised fashion [13], and the feedback of accuracy information can further enhance learning [10], [14]. One problem of the backpropagation is that it seems difficult to extract plentiful local features from few shots of input patterns. In this paper, we revisit and improve Hebbian learning, a local correlation-based learning rule that has inspired a large body of works on learning systems and synaptic plasticity. One key mechanism it relies on is activity-dependent synaptic modification first proposed by Hebb, simply phrased as ‘cells that fire together wire together’. Although experimental evidences such as long-term potentiation and depression [10], [15] support Hebbian-like rules, they are typically believed not practical and efficient in training artificial neural networks, compared to the backpropagation algorithm. It is our belief and the motivation of this paper that the potential of the Hebbian-learning approach has been underestimated.

Competition is the key of Hebbian learning to train a neural network. The motivation is that when each neuron in a layer tries to compete to fire while inhabiting the other neurons, the network is prone to convey the most information to the next layer. The reason that Hebbian learning hasn’t become practical is probably that much less

H. Zhou is with the School of Information Science and Engineering, Shandong University, Qingdao, Shandong, 266237 China. Email: hongchao@sdu.edu.cn.

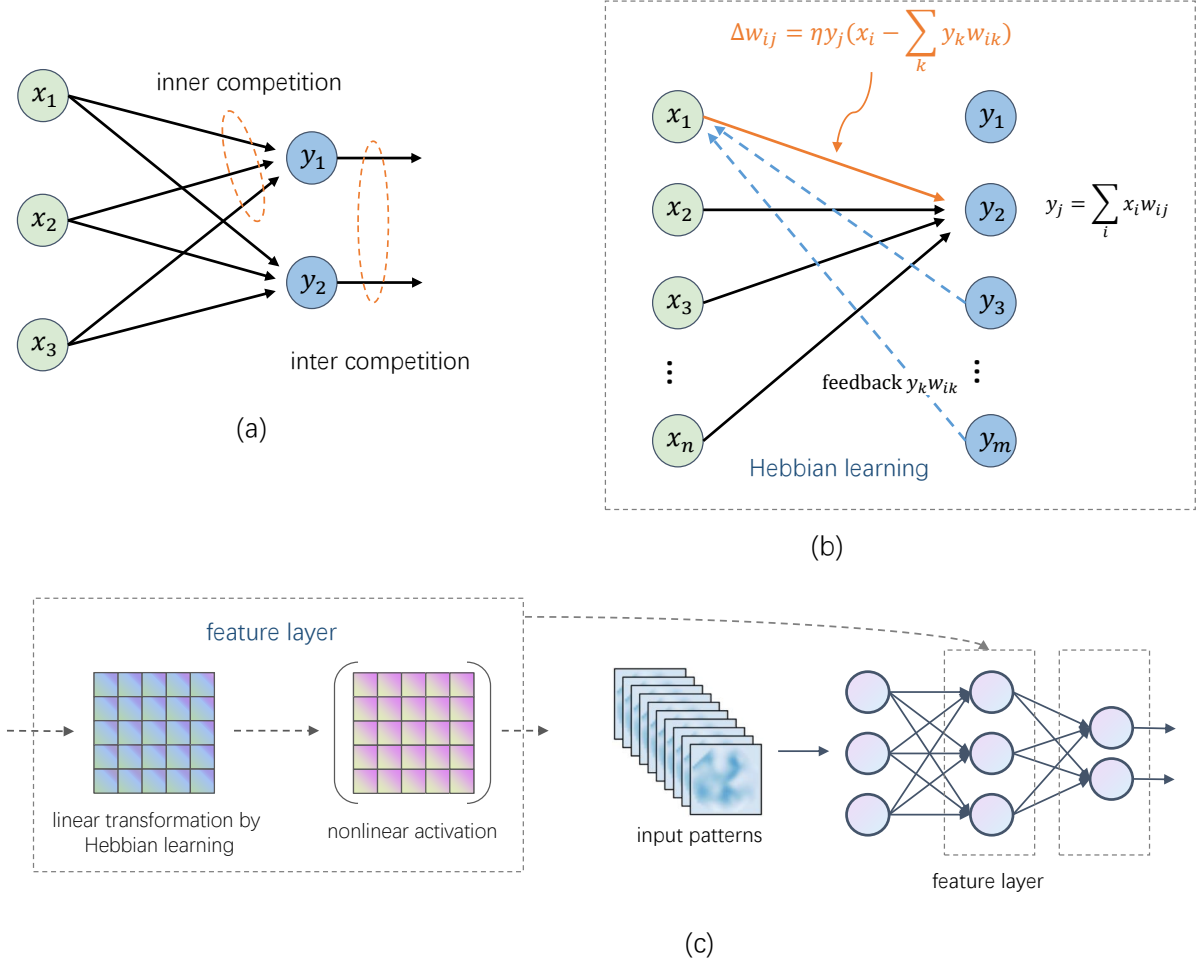


Fig. 1. Bottom-up unsupervised Hebbian learning. (a) Two types of competitions exist in neural networks - the competitions of the synapses of a neuron and the competitions of the neurons in the same layer to activate. (b) The Hebbian learning rule that raises local competitions and forces the neurons to learn different features. (c) A neural network with multiple layers for bottom-up unsupervised Hebbian learning, in which each layer consists of a linear transformation trained by the local Hebbian learning rule and a nonlinear activation transformation.

is known about the competition mechanism that forces different neurons to compete with each other [16]. There are two types of competitions - inner-neuron competitions and inter-neuron competitions, see Fig. 1(a). Within a neuron, when some synapses to a given postsynaptic neuron are strengthened, other synapses will be weakened [17], [18], with evidence from many biological systems [19], [20]. To raise competition among synapses of a neuron, constraints are introduced into various Hebbian learning models [21], such as limiting the synaptic strength sum of a neuron. Such constraints can be realized locally through some mechanisms, such as spike-timing-dependent synaptic plasticity [22], activity-dependent synaptic scaling [23], [24] and the sliding threshold of the BCM model [25].

Accumulating evidence reveals the crucial role of the second type of competitions, i.e. the competitions among neurons, in shaping learning activity [26], [27] - such competitions force neurons to represent different features.

In the cerebral cortex, a class of neurons called inhibitory neurons constitute about 20% of the cortical neuronal population [28]. When inhibitory neurons are activated, they release the transmitter GABA that makes the other neurons more difficult to fire, thus inhibiting their activation. Sparsity was exploited [16], [29]–[32] to model and raise competition among neurons in a layer. For example, relying on the assumption that neighboring neurons tend to excite each other and neurons at a greater distance tend to inhibit each other [33], [34] in a two-dimensional neuron layer, sparsity is used to model refinement of map-like cortical representation [35]. A popular competitive learning mechanism is ‘winner takes all’ [16] that divides the neurons in a layer into a group of inhibitory clusters, in which only the neuron with the strongest sum of synaptic input in each cluster is excited, thus inhabiting other neurons in that cluster. The competition mechanism of ‘winner takes all’, combined with biologically plausible synaptic modification, has recently attracted increasing attention [36]–[42], and demonstrated the possibility of achieving comparable performance to that of the backpropagation algorithm based on Hebbian-like learning rules. However, they impose a global-inhabitation constraint that only one neuron excited in a layer, which may limit the network’s expressive ability from information theoretic interpretation [43]. They also face the difficulty of working with neural networks of more than two hidden layers to discover hierarchical features.

We present an improved Hebbian learning rule for connection weight modification that injects competition within and among neurons. Specifically, the connection weight w_{ij} between neuron i in a layer and neuron j in the layer above is modified by

$$\Delta w_{ij} = \eta y_j (x_i - \sum_k y_k w_{ik}), \quad (1)$$

with x_i the output of neuron i as an input to neuron j , $y_j = \sum_u x_u w_{uj}$ the weighted sum of the input for neuron j , and η the learning rate. In this rule, the term $\sum_k y_k w_{ik}$ (summing over all neurons in the same layer with neuron j) for synaptic weight decay is the key to raise local competitions, as illustrated in Fig. 1(b). It can be decomposed as two terms $y_j w_{ij}$ and $\sum_{k \neq j} y_k w_{ik}$. The term $y_j w_{ij}$ previously studied in Oja’s rule [44] serves to limit the total synaptic weights over neuron j , thus raising competition among the synapses of a neuron. The term $\sum_{k \neq j} y_k w_{ik}$ further introduces competitions between neuron j and the other neurons, enabling neurons in the same layer to compete representing different features. Asymptotic analysis reveals that the learning rule approximately transforms an input pattern to some non-orthogonal principal components, and the feature learned can reconstruct the data in the layer below by simply multiplying the transpose of the weight matrix. This reconstruction capability makes the learning rule more resistant to adversarial attack [45]. With this learning rule, one can build a bottom-up network structure that extracts features from high dimensional input data, trained without supervision, see Fig. 1(c). This network structure can serve as a pre-training model to improve the performances of some supervised learning tasks. It may also drive the advances of neuromorphic hardware [46] as this learning rule is easier to implement for on-chip training. More attractively, this local learning rule enables us to build a new learning paradigm very different from the backpropagation for neural networks, named activation learning, where the output activation of the neural network roughly measures how probable the input patterns are, simply phrased as ‘learn more, activate more’.

In activation learning, each layer is trained by the proposed local Hebbian learning rule, and the activation

function of each layer is a nonlinear mapping that preserves the magnitude (l_2 norm) of the outputs. The inference is to retrieve the missing units of the input patterns that maximize the output activations, i.e., to find the most probable patterns. Naturally, it can serve as both the discriminative and generative models, with the same trained neural network that takes both the data and the category as input. A discriminative model is to infer the missing category from the data, and a generative model is to infer the data from a given category while injecting some randomness. Our experiments on MNIST demonstrate that the activation learning outperforms the backpropagation algorithm when the number of training samples is relatively small. For example, in the case of 600 labeled training samples, the activation learning achieves about 9.74% classification error rate on MNIST, while the backpropagation achieves 25.5% error rate. And with the help of a pre-training model trained based on 60000 unlabeled images, the error rate of the backpropagation can be reduced to 20.3%, which is still much higher than that of the activation learning trained only based on 600 labeled images. This is because that the activation learning can learn plentiful local features from many small pieces of each input pattern, but the backpropagation can only learn from the single scalar of global loss. It is also demonstrated that the activation learning is robust against external disturbances, such as partially masking or adding some noise lines that have not been learned by the model. The performance of the activation learning can be further enhanced with the feedback of accuracy information, which for example introduces a reward that modulates the global learning rate. In addition, compared to the network with full connections, local connections without parameter sharing can not only reduce the size of the parameters and the computational cost, but also stabilize learning and improve the network performance, illustrated by experiments on CIFAR.

The rest of this paper is organized as follows. Section II introduces the improved Hebbian learning rule that raises competition among neurons, and analyzes its converged properties. Section III investigates and evaluates the features learned by the local learning rule without supervision. Section IV presents the framework of activation learning and conducts experiments for classification on MNIST. Section V studies the activation learning as a generative model. Activation learning with local connections is investigated in Section VI, with some experiments on CIFAR. Section VII further discusses the potential and some challenges of activation learning as a general-task model, followed by conclusions.

II. LEARNING BY LOCAL COMPETITIONS

A. Hebbian Learning Rule

Hebb's proposal for learning is to modify the connection weights of neurons, following the principle of 'cells that fire together wire together.' The connection weight w_{ij} between a neuron i in a layer and neuron j in the layer above increases if the two neurons fire simultaneously. Formally, the original version of Hebbian learning is

$$\Delta w_{ij} = \eta x_i y_j \quad (2)$$

with x_i the output of neuron i as an input to neuron j , y_i the output of neuron j , and η the learning rate. But this original version is not stable in learning: all the weights may grow unboundedly until reaching their maximum allowed values, hence not practically useful.

To guarantee the convergence of Hebbian learning, a constraint that conserves the total synaptic weight of a neuron can be enforced through synaptic weight decay [21] to control the total increase. A modified version proposed by Oja [44] is

$$\Delta w_{ij} = \eta y_j (x_i - y_j w_{ij}), \quad (3)$$

where the net input $y_j = \sum_i x_i w_{ij}$ is the weighted sum of the input. This rule imposes competitions among the synaptic weights of a neuron and re-config those weights through training. However, this rule was designed for the training of a single neuron. In order to work with multiple neurons in a layer, this rule must be modified or combined with other constraints (such as ‘winner takes all’) to force the neurons to compete.

In this paper, we develop the following Hebbian local learning rule, which imposes competitions within neurons and among neurons:

$$\Delta w_{ij} = \eta y_j (x_i - \sum_k y_k w_{ik}), \quad (4)$$

with the net input $y_j = \sum_u x_u w_{uj}$. In this rule, the input x_i is adjusted by an internal feedback from all the receiving neurons, i.e., $\sum_k y_k w_{ik}$. This feedback term can be decomposed into two parts, the feedback $y_j w_{ij}$ from neuron j and the feedback $\sum_{k \neq j} y_k w_{ik}$ from the other receiving neurons. The feedback from neuron j , the same as the learning rule (3), results in the control of the total synaptic weights of neuron j . The feedback from the other receiving neurons forces them to compete with neuron j to fire. To see this, if another receiving neuron k excites, the connection w_{ij} to neuron j is weakened by a magnitude of $\eta y_j y_k w_{ik}$ (assuming all the variables are positive) contributed by neuron k ’s excitation. As a result, highly correlated neurons inhibit each other to activate, and different neurons are forced to have different combinations of connection weights. If we treat the feedback term $\sum_k y_k w_{ik}$ as a reconstruction of x_i , the rule acts to learn from the error of the reconstruction, forcing the reconstruction to approximate the input.

B. Stable Solution Analysis

We analyze the converged properties of the local learning rule (4), starting with the study of its dynamics. First, the net input of the neurons in a layer is a linear transformation of the input pattern, written as

$$\mathbf{y} = \mathbf{w}^T \mathbf{x} \quad (5)$$

with $\mathbf{y} = [y_1, y_2, \dots]$ the vector of the net input, $\mathbf{x} = [x_1, x_2, \dots]$ the vector of the input, and \mathbf{w} the matrix of the connection weights.

Then the learning rule (4) can be rewritten as

$$\Delta \mathbf{w} = \eta (\mathbf{x} \mathbf{x}^T \mathbf{w} - \mathbf{w} (\mathbf{w}^T \mathbf{x} \mathbf{x}^T \mathbf{w})). \quad (6)$$

With a very small learning rate η , the dynamics of \mathbf{w} can be approximated by a differential equation

$$\frac{d\mathbf{w}}{dt} = C \mathbf{w} - \mathbf{w} (\mathbf{w}^T C \mathbf{w}), \quad (7)$$

where \mathbf{w} is for $\mathbf{w}(t)$ as a time-dependent matrix, and $C = E\{\mathbf{x}\mathbf{x}^T\}$ is the covariance matrix of the training samples. The matrix C is positive semidefinite, i.e., all its eigenvalues are positive. Through enough number of modification steps, the connection weights \mathbf{w} tend to converge to asymptotically stable solutions of (7) specified by

$$C\mathbf{w} - \mathbf{w}\mathbf{w}^T C\mathbf{w} = 0. \quad (8)$$

When the number of receiving neurons $m \geq 2$, there are infinite of stable solutions. The learning rule (4) converges to which stable point depends on the initial starting value of \mathbf{w} , the training input patterns, and the learning rate. From the condition (8) of the stable solutions of the proposed learning rule, we can get several results to help us understand some mechanisms under the learning rule.

Result 1 (Reconstruction Error): The learning rule (4) performs to approximately minimize the mean reconstruction error

$$E\|\mathbf{x} - \mathbf{w}\mathbf{w}^T \mathbf{x}\|^2, \quad (9)$$

in which $\mathbf{w}\mathbf{w}^T \mathbf{x} = \mathbf{w}\mathbf{y}$ can be considered as a reconstruction of \mathbf{x} . It follows that the gradient of this reconstruction error with respect to \mathbf{w} equals to 0 when \mathbf{w} is a stable solution satisfying (8), proved by Appendix-A. This implies that the learning rule tries to decompose the input pattern \mathbf{x} into m components with a minimum mean reconstruction error.

Result 2 (Single Neuron): With a single receiving neuron, i.e., $m = 1$, the learning rule (4) becomes Oja's rule (3), and it performs the same as the principal component analysis (PCA) [44]. In this case, the connection weights \mathbf{w} is a vector and it converges to the normalized eigenvector corresponding to the largest eigenvalue of the covariance matrix C (either of the two possible choices), denoted by \mathbf{v} . If the initial connection weights $\mathbf{w}^T(0)\mathbf{v} > 0$, \mathbf{w} tends to converge to \mathbf{v} , otherwise converge to $-\mathbf{v}$.

Result 3 (Connection to PCA): For any stable solution \mathbf{w} with $m > 1$, the reconstruction error (9) is equal to that of the principal component analysis (PCA) with m components, proved by Appendix-B. This implies that the learning rule (4) performs similar to PCA, which guarantees that as much information as possible is passed to the next layer. Existing works have demonstrated that PCA can be used to extract features of network layer [47]. But unlike PCA, orthogonality is unnecessary and usually does not meet the stable solutions of our learning rule. It is not desirable to use the original PCA to extract features in a layer, because the neural network may become vulnerable to the failure of a few neurons corresponding to the biggest eigenvalues, and it is also difficult to achieve perfect orthonormalization with a local learning rule.

Result 4 (Stable Solutions): There are infinitely many stable solutions of (7) that form a surface when the number of neurons $m > 1$. Let $\mathbf{v}_1, \mathbf{v}_2, \dots, \mathbf{v}_m$ be the normalized eigenvectors corresponding to the m largest eigenvalues of C , then the weight matrix \mathbf{w} is a stable solution if and only if for any $1 \leq j \leq m$, the j th column (the weights of neuron j) of \mathbf{w} can be written as

$$\mathbf{w}_j = u_{j1}\mathbf{v}_1 + u_{j2}\mathbf{v}_2 + \dots + u_{jm}\mathbf{v}_m \quad (10)$$

with some $\{u_{jk}\}$ such that $u_{1k}^2 + u_{2k}^2 + \dots + u_{mk}^2 = 1$ for all $1 \leq k \leq m$ (the factors associated to each eigenvector \mathbf{v}_k is normalized), see the proof in Appendix-C. As a consequence, $\|\mathbf{w}\| = \sum_{ij} w_{ij}^2$ tends to converge to m even

though there is no explicit constraint or normalization in the learning rule. This result leads us to the observation that changing any column \mathbf{w}_j to $-\mathbf{w}_j$ does not affect the stability of a solution \mathbf{w} .

Result 5 (Activation Bound): A property of the learning rule (4) is that the output activation $\|\mathbf{y}\|^2 = \sum_j y_j^2 = \|\mathbf{w}^T \mathbf{x}\|^2$ tends to be upper bounded by the input strength $\|\mathbf{x}\|^2$. Let \mathbf{w}_j be the j th column of \mathbf{w} , Appendix-D derives that in each modification step of the learning rule (4)

$$\Delta(y_j^2) \leq y_j^2(\|\mathbf{x}\|^2 - \|\mathbf{y}\|^2) + O(\eta^2). \quad (11)$$

As long as $\|\mathbf{y}\|^2$ is larger than $\|\mathbf{x}\|^2$, $\Delta(y_j^2)$ is smaller than 0, driving $\|\mathbf{y}\|^2$ towards smaller than $\|\mathbf{x}\|^2$.

Result 6 (Activation as Typicality): Given a layer trained by the learning rule (4), we observe that if fixing the input strength $\|\mathbf{x}\|^2$, a more probable input likely induces higher output activation $\|\mathbf{y}\|^2$. This implies that the amount of the output activation may be used to approximate how typical the input pattern is.

To explain the intuition behind this, we assume that m is smaller than the input dimension and denote V the vector space spanned from the eigenvectors $\mathbf{v}_1, \mathbf{v}_2, \dots, \mathbf{v}_m$ corresponding to the largest eigenvalues of the covariance matrix $C = E\{\mathbf{x}\mathbf{x}^T\}$. We call V the typical space. Let $d(\mathbf{x}, V)$ be the distance of \mathbf{x} to the typical space V , then

$$d(\mathbf{x}, V) = \sqrt{\|\mathbf{x}\|^2 - \sum_i \|\mathbf{x}^T \mathbf{v}_i\|^2}. \quad (12)$$

We find that, in Appendix-E, $\|\mathbf{y}\|^2$ tends to be upper bounded by

$$\|\mathbf{x}\|^2 - d^2(\mathbf{x}, V). \quad (13)$$

For the special case that $\mathbf{w} = [\mathbf{v}_1, \dots, \mathbf{v}_m]$, $\|\mathbf{y}\|^2$ converges to $\|\mathbf{x}\|^2 - d^2(\mathbf{x}, V)$. Therefore, the output activation $\|\mathbf{y}\|^2$ approximately measures how close the input \mathbf{x} is from the typical space V , named the typicality of \mathbf{x} . Although the case where m is less than the input dimension is discussed, the conclusion holds for general m , which motivates the emergence of the activation learning.

C. Network Training

The learning rule (4) naturally fits for the bottom-up unsupervised neural network training. Given a neural network, as shown in Fig. 1(c), each layer trained by the local Hebbian learning rule extracts features from the data of the lower layer, following a chain rule for the multiple layers. A nonlinear activation function is applied to the net input to get the output of each layer. Generally, neurons in the lower layer represent low-level features and neurons in the higher layer represent high-level features.

To implement the local learning rule, the training samples can be shuffled and organized into batches to train the network. The learning rule (4) can be modified as

$$\Delta w_{ij} = \eta \sum_{b \in \text{batch}} y_j^b (x_i^b - \sum_k y_k^b w_{ik}), \quad (14)$$

where index b enumerates the input samples in a given batch, x_i^b represents the i th unit of the b th input sample, and the net input $y_j^b = \sum_i x_i^b w_{ij}$. The weights are updated with each batch for a certain number of epochs. A network of multiple layers can be trained layer by layer, or all the layers can be trained together.

Compared to the backpropagation algorithm, the Hebbian learning rule is more capable of discovering plentiful features from local pieces based on few shots of samples. An application of the local learning rule is to generate an unsupervised pre-training model that extracts high-quality features and can be later fine-tuned with the help of supervision. Such a pre-training model has the potential to boost the performance of some learning tasks, or reduce the requirement for the amount of labeled data. What is more attractive is that this Hebbian learning rule enables us to create a new learning paradigm, called activation learning, which unifies supervised learning, unsupervised learning and generative models. It shows excellent performance in low sample complexity. Because the underlying learning rule aims at exploring inherent correlations of the input patterns independent of specific tasks, the resulting models can be used for general purposes and can work with a wide range of learning tasks.

III. UNSUPERVISED FEATURE LEARNING

Before studying activation learning, in this section we investigate and evaluate the features learned by the local learning rule without supervision, by conducting experiments on the MNIST dataset, which is a database of black-and-white handwritten digit images with 28×28 pixels each. In the experiments, a dense neural network of l feature layers with each layer consisting of 28×28 neurons is trained based on 55000 normalized training images without labels. The square $(\cdot)^2$ is used as the activation function to make strong activation stronger, and it is then normalized so that the feature of each layer is a unit vector, as shown in Fig. 2(a). The connection weights are initialized from a normal distribution of zero mean and small variance, and are iteratively updated according to the Hebbian learning rule (14) with batch size 100. The network is trained layer by layer in a bottom-up manner - when one layer finishes training, its connection weights are frozen and the training of the next layer begins.

A. Unsupervised Features

We conduct experiments to examine the features learned by the unsupervised Hebbian learning rule (4), and compare them with those learned by backpropagation based on the same neural network connected to 10 output units on top, whose softmax is used as the predicted probability distribution of the input digit. Fig. 2(b) plots the features of the 36 most excited units in the first layer learned by the Hebbian learning rule, where the white color represents positive values, the blue color represents negative values, and the black color represents zeros. The features are obtained by calculating the gradient of the target unit with respect to the input image, reflecting whether an image pixel excites the target unit or inhabits it. Fig. 2(c) plots the features of the second layer learned by the Hebbian rule, which look less speckled than those of the first layer. Each feature pattern of the second layer consists of some spots, reflecting statistically correlated pixels of input images. The features are near zero at the periphery of the images, as the pixels on the periphery of the images are usually uninformative. In fact, the features of each layer learned by the Hebbian learning rule is capable to reconstruct the data in the layer below, this makes the neural networks more resistant to adversarial attack [45]. We see that the features learned by the Hebbian learning rule are very different from those learned by backpropagation shown in Fig. 2(d). The features developed by backpropagation look more random in shape, and spread out over the entire images. With those non-zero features associated with periphery pixels, the neural network is easily deceived by the generated adversarial

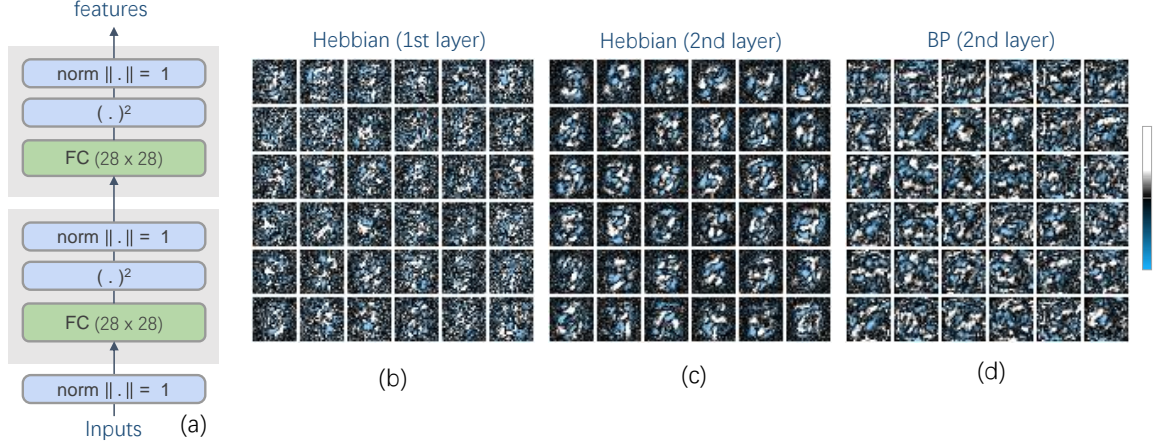


Fig. 2. Learning features from MNIST by the Hebbian rule and the backpropagation (BP) algorithm respectively. (a) Network structure with two feature layers. (b) The features of the 36 most excited units in the first layer learned by the Hebbian learning rule. The white color represents positive values and the blue color represents negative values, reflecting whether the input pixel excites or inhibits the targeting neuron unit. (c) The features of the second layer learned by the Hebbian rule. (d) The features of the second layer learned by backpropagation, based on the same network structure connected to 10 output units on top, whose softmax is used as the predicted probability distribution of the input digit. .

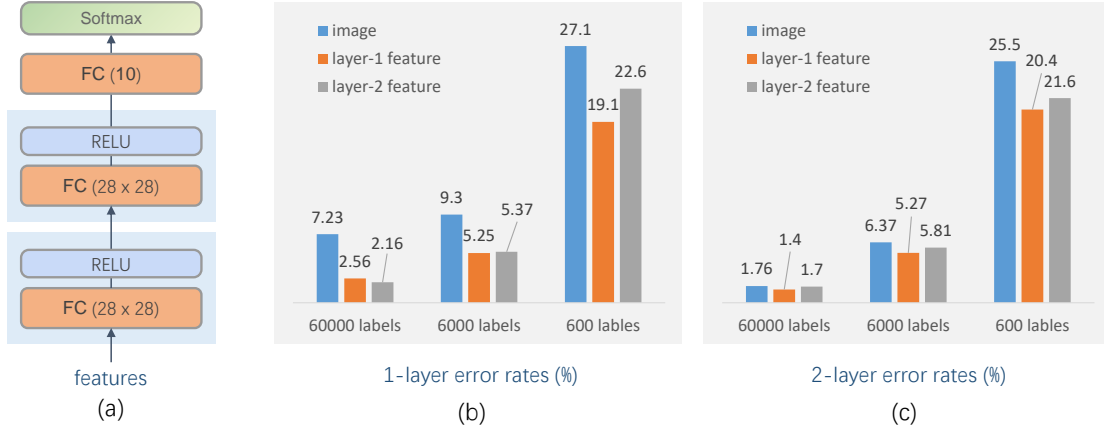


Fig. 3. Classification based on the unsupervised features learned by the Hebbian rule on MNIST. (a) The classification network that takes the learned features as the input and is trained by backpropagation. (b) The test classification error rates of the network that has only a single layer and is trained by backpropagation based on 60000, 6000, or 600 labeled images respectively. It compares three cases: taking the normalized images as the input, taking the first layer features as the input, and taking the second layer features as the input. (c) The classification error rates of the network with two layers that is trained by backpropagation.

images [38]. This further supports that the Hebbian learning rule (4) is potentially more secure to learn features against adversarial attack.

B. Classification on Features

To evaluate the features learned without supervision, they are used as input to the classification task, compared to using the original images as input. The neural network used for classification is a fully connected network, which

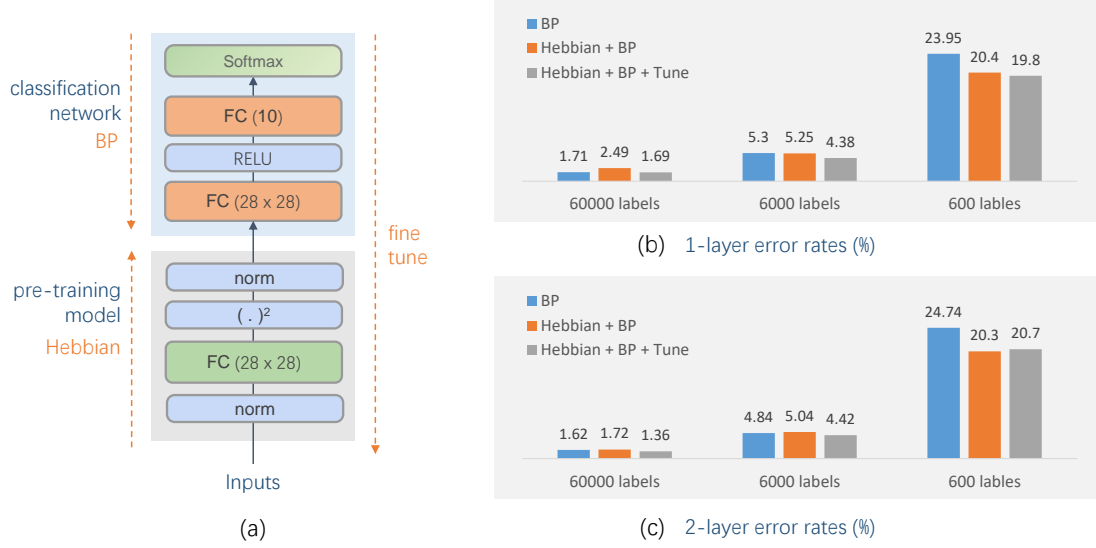


Fig. 4. Hebbian learning as a pre-training model. (a) A network structure that consists of a pre-training model and a classification network on top. (b) The test classification error rates of the network with only one layer on top of the pre-training model. It compares three different training methods for a given number of labeled images. (c) The test classification error rates of the network that has two layers on top of the pre-training model.

consists of some hidden layers and one output layer of 10 units, see Fig. 3(a). Each hidden layers has 28×28 neurons and uses RELU as the activation function. The softmax of the ten output units is used as the predicted probability distribution of the digit of the input image, and the classified digit is the one with the largest softmax value. The neural network used for classification is trained by backpropagation, on 60000 images, 6000 images, and 600 images respectively, in which 5000, 1000 and 100 images are used for validation.

Fig. 3(b) shows the test classification error rates of a neural network without hidden layers, which takes the learned features or the original images as the inputs. When there are 60000 labeled images, directly using the original images as the inputs leads to a test error rate of 7.23%, which can be reduced to 2.56% if using the 1st-layer features learned by the Hebbian rule as the inputs. Because the proposed learning rule aims to extract correlations from the input patterns in a general way, the trained network can be used to preprocess input data for a wide range of learning tasks. If we further replace the 1st-layer Hebbian features with the 2nd-layer features, the classification accuracy may decrease slightly, partly due to the loss of information in feature extraction. A similar phenomenon can be observed when using a neural network of two layers, as shown in Fig. 3(c). With 60000 labeled images, we see that the 2nd-layer features lead to a worse performance than the 1st-layer features in the classification task.

C. Pre-training Model

The network trained by the Hebbian learning rule can also be used as a pre-training model, which is fine-tuned in the future by backpropagation for some specific learning tasks. The fine-tuning helps to reshape the unsupervised

features in order to better adapt to the target task. In the experiments, the used neural network consists of two parts - a pre-training model and a classification network, as shown in Fig. 4(a). Based on which, we conduct a group of experiments on MNIST, and compare the performances of three different training methods: (1) training the entire network by backpropagation; (2) training the pre-training model based on all the 60000 images without using their labels by the Hebbian learning rule, and then training the classification network by backpropagation; and (3) fine-tuning the entire network by propagation based on the one trained by the second method.

Fig. 4(b) and (c) give the test error rates when the classification network has a single layer or two layers, respectively. We see that given all the 60000 images labeled, the second method results in a higher classification error rate than the first method that trains the whole network by backpropagation. But when the number of labeled images is reduced to 600, the second method leads to significantly better performance. For almost all the experiments, the third method with fine-tuning performs the best. This confirms that the unsupervised features learned from a large amount of unlabeled data are helpful to a supervised learning task, and supervised information can be used to adjust the features and enhance learning. Our goal here is not to surpass the state of art on MNIST, but to show that the performance of the backpropagation can be further improved with the help of unsupervised Hebbian learning.

IV. ACTIVATION LEARNING

It is believed that the brain learns in a predominantly unsupervised fashion [13], [48], and it is unclear how unsupervised learning and supervised learning are integrated in the brain. Considering the scenario of learning a digit, in which the brain receives both the visual and voice signals of the digit. The brain is unlikely to manually select the voice signal as the label and the visual signal as the data. Instead, it may take both the signals as the input, and create their association in an unsupervised way that enables retrieving the vocal signal from a visual input and vice versa. The *activation learning* follows this idea. It tries to explore correlations within any input patterns based on the Hebbian learning rule, and its output activation approximately estimates the typicality of the input pattern. In addition, the brain is a system of general intelligence that handles very different tasks, but the backpropagation algorithm seems too task-specific, that is, for every learning task it has to design a specific loss function to optimize. By comparison, the activation learning aims at learning the statistical distribution of the training samples independent of any specific tasks, and can be used as a general task model. This section conducts experiments on MNIST to learn some aspects of the activation learning for discrimination.

A. Paradigm of Activation Learning

The proposed Hebbian learning rule enables us to establish the new learning paradigm of activation learning, in which training is performed based on the local learning rule through feedforward and local feedback, and inference is to retrieve the missing units of the input pattern to maximize the output activation. It follows Result 6 of the Hebbian learning rule, that is, the output of a layer trained by the local learning rule tends to activate more on a more probable input.

Activation learning can take both the data and the labels as input, and process them through multiple layers trained by the Hebbian learning rule, as illustrated in Fig. 5(a). In order to control the output activation, the activation

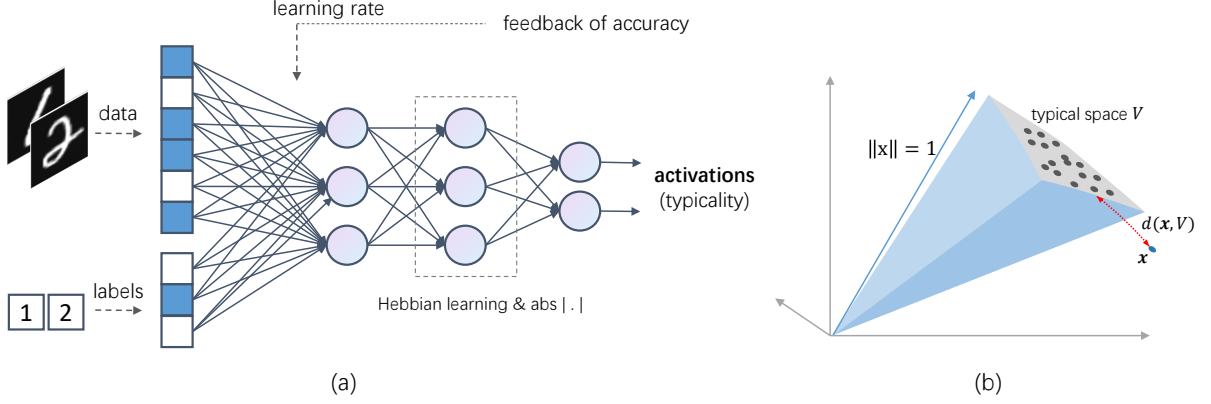


Fig. 5. The paradigm of activation learning. (a) A neural network that takes both the data and labels as the input consists of multiple layers with each layer trained by Hebbian learning and using a nonlinear magnitude-preserving function as the activation function. (b) The output activation approximately measures how close the input pattern is to a typical space. The closer the input pattern is, the stronger the output activation is.

function of each layer is required to maintain the magnitude of the input, i.e., it is a nonlinear function f such that $\|f(\mathbf{y})\| = \|\mathbf{y}\|$ for any input \mathbf{y} . This allows cascading of the multiple layers so that the final output activation tends to decrease as the network gets deeper. An interpretation of the activation learning is given in Fig. 5(b). For a network with a single layer, the output activation roughly measures the distance of the input pattern to a typical linear space that spans from the eigenvectors corresponding to the largest eigenvalues of the co-variance matrix $C = \{\mathbf{x}\mathbf{x}^T\}$. By cascading multiple layers with nonlinear activation functions, the typical space is trimmed and reshaped to be nonlinear and compact, so that it can better describe the probability distribution of the input samples. A simple nonlinear activation function is the absolute value function $|\cdot|$. It simply folds the typical space without re-scaling or distorting the distance measurement, making the output activation a good estimate of how typical the input pattern is.

This framework of activation learning can easily unify supervised learning, unsupervised learning and semi-supervised learning. For supervised learning, see Fig. 5(a), a neural network of activation learning takes both the data and the label as the join input for training, different from a conventional neural network, which takes the data as the input and uses the label to calculate the output error. The input data with the correct label usually yields a stronger output activation than that with a wrong label. The process of inference is to find the best label that combines with the given input data to maximize the output activation. In many scenarios, labelling data is expensive, and it is found that the features learned from unlabeled data can be used to improve the performance of many learning tasks, thus leading to unsupervised learning and semi-supervised learning. In activation learning, supervised learning and unsupervised learning could be easily mixed together. When encountering data without labels, they can be directly fed to the network to adjust the related connection weights of neurons. These weights represent some features that are useful to a wide range of learning tasks such as classification. Meanwhile, when meeting data with labels, the supervised label information can help to reshape the unsupervised features and establish their association with the label.

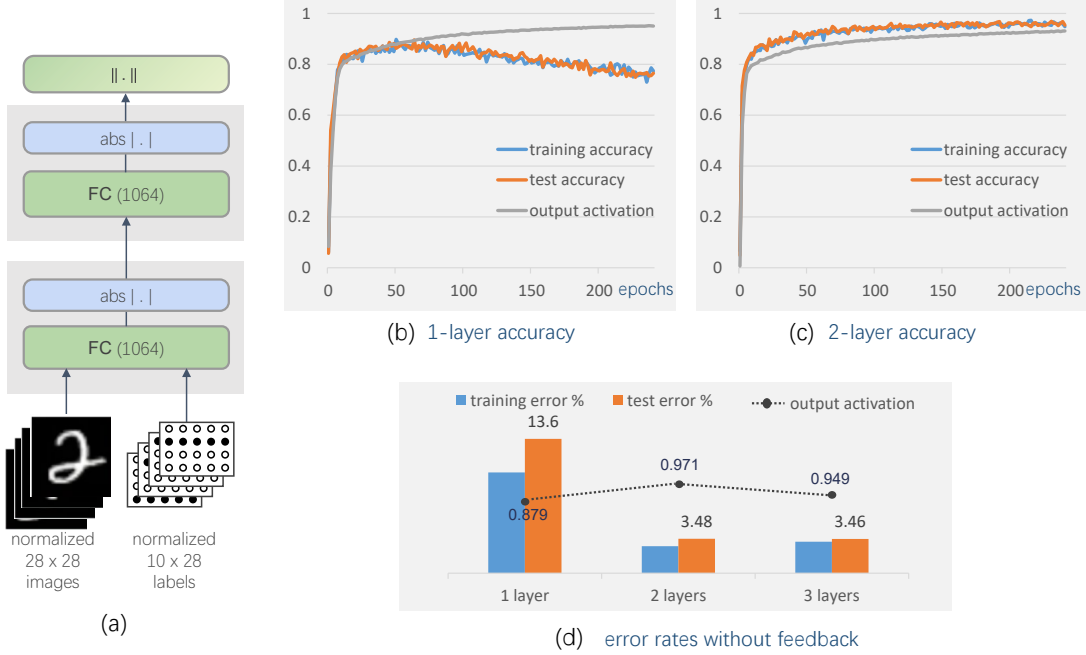


Fig. 6. Activation learning for classification on MNIST. (a) The network structure for activation learning on MNIST, which consists of h layers with $28 \times 28 + 10 \times 28$ units in each layer trained by the Hebbian learning rule, and using $|\cdot|$ as the activation function. (b) The training and test accuracy as training progresses for 1-layer network. (c) The training and test accuracy as training progresses for 2-layer network. (d) The test classification error rates of the activation learning without feedback of accuracy information, when the network has 1, 2 or 3 layers respectively. The dotted line indicates the corresponding normalized network output activation.

B. Classification without Feedback

We study the activation learning for classification based on all the 60000 training images with labels, in which 5000 images are used for validation. In the experiments, a simple network structure is used as shown in Fig. 6(a), which takes both the normalized 28×28 digit images and the normalized 10×28 encoded representations of their labels as inputs. The encoded representation of digit i is an 10×28 matrix in which all the units in the i th row are ones and the other units are zeros. This network consists of several layers with $28 \times 28 + 10 \times 28$ units in each layer (the same size as the input), trained by the Hebbian learning rule, and using the absolute function $|\cdot|$ as the activation function. When classifying a digit image, it tries to find the missing label representation that combines with the given input image to maximize the output activation. So given an input image \mathbf{a} , the optimal inferred digit representation is

$$\mathbf{z}^* = \arg \max_{\mathbf{z}} \|\mathbf{y}(\mathbf{a}, \mathbf{z})\|^2 \quad (15)$$

with \mathbf{y} the network output depending on the joint input (\mathbf{a}, \mathbf{z}) . A way of getting the optimal \mathbf{z}^* is to enumerate all the possibilities of the classes and choose the best one.

Fig. 6(d) shows the test classification error rates when the network has 1, 2 or 3 layers respectively. When the network has a single layer, see Fig. 6(b) for the training process, the test accuracy first increases and then monotonically decreases. The error rate reaches 13.6% when early stopping is applied. As the network becomes

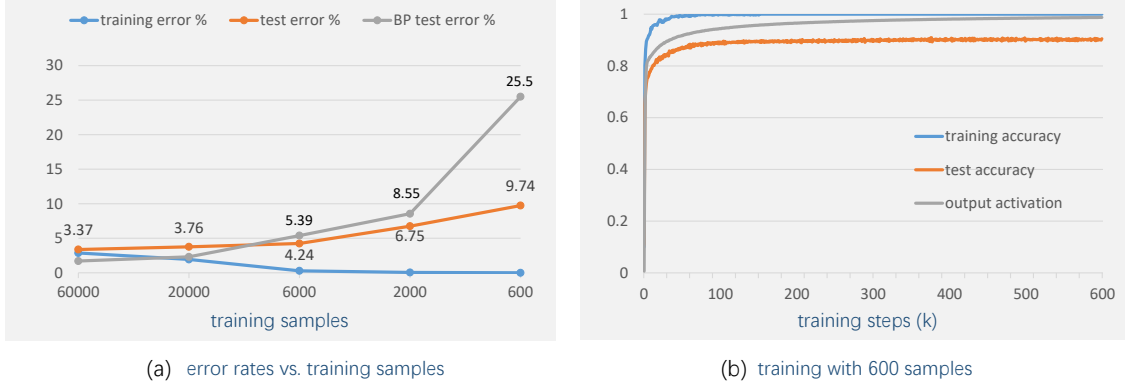


Fig. 7. (a) The classification error rates of the two-layer network trained by a certain number of labeled samples without feedback, compared to that of a three-layer network trained by backpropagation. (b) The training and test accuracies as training progresses based on 600 training samples.

deeper – from one layer to two layers, the error rate is reduced to about 3.48%. There seems to be a phase change from one layer to multiple layers: in the case of multiple layers, both the training and test accuracies tend to monotonically increase as training progresses, see Fig. 6(c). An interesting observation is that the training accuracy is very close to the corresponding test accuracy in the given number of training epochs, showing the excellent generalization ability of the activation learning.

C. Low Sample Complexity

Fig. 7(a) studies how the number of training samples affects the error rates of the activation learning with a two-layer network. We compare them with the classification error rates of a three-layer network trained by backpropagation, which has roughly the same level of model complexity (there is an exception: when the number of training samples is 600, a two-layer network trained by backpropagation is used for better performance). Note that when the sample complexity is low, overfitting occurs when a model is over-trained by backpropagation with a relatively small number of samples, resulting in performance degradation. In order to overcome this overfitting, 1/6 of the training samples are used for validation, and early stopping that minimizes the validation error rate is applied to the training by backpropagation. However, this early stopping as well as the monitoring of the validation error is not necessary for the activation learning of a multilayer network, as its test error rate tends to monotonically decrease in a very large number of training steps. In the figure, when the number of training samples is 60000, the test error rate of the activation learning is about 3.37%, which is not as good as the backpropagation. But when the sample complexity is reduced to 6000, the activation learning outperforms the backpropagation. If the sample complexity is further reduced to 600, the test error rate of the activation learning will increase to about 9.74%, but the error rate of the backpropagation will reach as high as 25.5%. It demonstrates that the activation learning can significantly outperform the backpropagation when the number of training samples is small. It also works better than the approach of using a pre-training model described in the previous section. When the pre-training model is

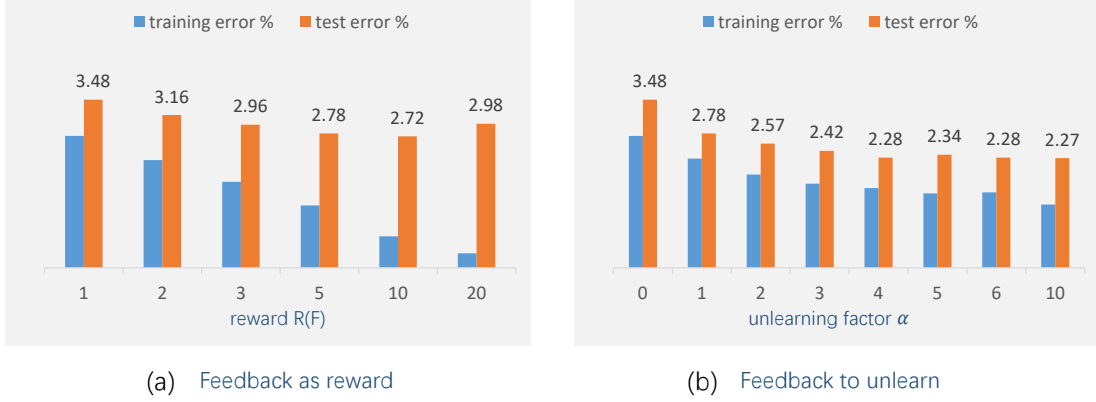


Fig. 8. Activation learning with feedback on MNIST. (a) The classification error rates of the model trained with feedback that introduces a reward $R(F)$ to modulate the learning rate. (c) The classification error rates of the model that unlearns the negative samples obtained from feedback.

trained by 60000 unlabeled images and then fine-tuned by 600 labeled images, its error rate is about 20.3%, while the activation learning achieves an error rate of 9.74% only based on 600 labeled images.

Surprisingly, even if the sample complexity is very low, the test error rates of the activation learning in our experiments do not increase as training progresses, which is very different from most learning methods including those based on backpropagation. Fig. 7(b) shows the training and test accuracies as training progresses when the sample complexity is 600. The training accuracy quickly converges to 1 due to the small number of training samples, and the test accuracy keeps slowly increasing even at the end of the training steps. This is unusual, and the activation learning performs more resistant to overfitting - one does not need techniques such as regularization or early stopping to combat overfitting. Activation learning appears to be a powerful learning paradigm to work with a relatively small number of training samples.

D. Learning with Feedback

The feedback of accuracy information plays an important role in enhancing human learning [10], [14] observed in some learning experiments, probably by providing something more than the simple correlation-based strengthening of synaptic connections.

In order to introduce accuracy feedback into activation learning, we modify the learning rule (4) so that a feedback signal introduces a reward that modulates the learning rate:

$$\Delta w_{ij} = \eta R(F) y_j (x_i - \sum_k y_k w_{ik}), \quad (16)$$

in which $R(F)$ is a global reward for the whole network, as suggested in [10]. For classification tasks, we let $R(F) = 1$ for the correctly classified training samples, and let $R(F) > 1$ for the incorrectly classified training samples. It is equivalent to learning more times on the incorrectly classified samples. When $R(F)$ is sufficiently large, the rule becomes learning only from errors. Fig. 8(a) shows the classification error rates of the two-layer

network with different feedback rewards, that is $R(F) = 1, 2, 5, 10, 20$ respectively. Given all the trained images labeled, we see that the classification error rate can be reduced to 2.72% as $R(F)$ increases to 10.0.

In the above method, the training only performs on the positive training samples that are correctly labeled. This makes their output activations usually stronger than those with incorrect labels. If one can further unlearn the negative samples with incorrect labels, it will increase the gap between the positive samples and the negative samples on the output activations, hence achieving a better classification. Specifically, given a training sample (\mathbf{x}_i, l_i) with \mathbf{x}_i the data and l_i the correct label, we treat it as a positive sample, and create a negative sample (\mathbf{x}_i, l'_i) with $l'_i \neq l_i$ the wrong label that yields the highest output activation. In order to distinguish them, a model should not only encourage the positive sample to excite, but also inhabit the negative sample when their gap is small.

Let Δw_{ij}^+ be the modification of the connection weights based on the learning rule (4) when giving a positive sample (\mathbf{x}_i, l_i) , and let Δw_{ij}^- be the change of the connection weights for the negative sample (\mathbf{x}_i, l'_i) . We study a learning rule such that the resulting change of the connection weights at a training step is

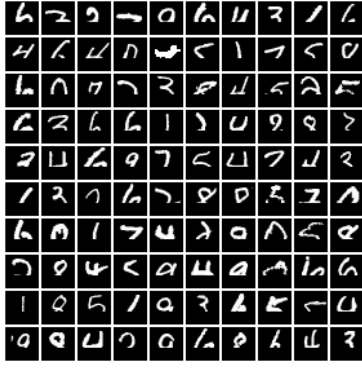
$$\Delta w_{ij} = \Delta w_{ij}^+ + R(g)(\Delta w_{ij}^+ - \Delta w_{ij}^-), \quad (17)$$

where $R(g) \geq 0$ depends on the gap between the positive sample and the negative sample, and $R(g)(\Delta w_{ij}^+ - \Delta w_{ij}^-)$ performs to increase the gap. In our experiments, it chooses $R(g) = \alpha$ for a positive constant α (referred as the unlearning factor) when the gap $\|\mathbf{y}(\mathbf{x}_i, l_i)\|^2 - \|\mathbf{y}(\mathbf{x}_i, l'_i)\|^2 < 0.1$, and otherwise $R(g) = 0$. Fig. 8(b) studies how the value of α affects the classification error rates on MNIST. When $\alpha = 4.0$, it achieves the error rate of about 2.28%, outperforming the previous method that takes the feedback as a reward. It is comparable to the human accuracy (the error rate around 2%-2.5% [49]) on the MNIST data.

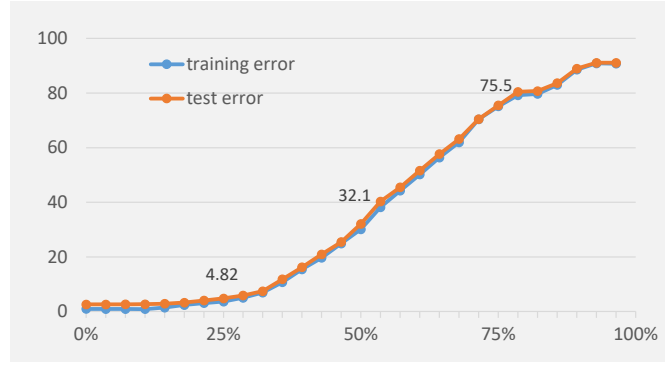
E. Classification on Incomplete Images

We continue working with the previously trained two-layer neural network, and study the activation learning's ability in recognizing incomplete or disturbed images. In the first group of experiments, given some images from MNIST, we mask their bottom parts ($a \times 28$ pixels) as black (zeros), and recognize the digits based on the known parts at the top, see Fig. 9(a). In this scenario, it directly takes the masked images as the input, and infers the digits by searching the optimal solutions that maximize the output activations. Fig. 9(b) gives the error rates for different masking ratios, namely, the fraction of pixels being masked in each image that is $a/28$. It shows that when the masking ratio is less than $1/3$, the classification error rate is less than 8%; it quickly grows to 32.1% when the masking ratio increases to 50%. In fact, if we look at the sampled masked images in Fig. 9(a), there are a certain number of images very difficult to recognize. Overall, activation learning has demonstrated a certain ability to tolerate some parts of the input patterns being covered or missed in image recognition.

We also conduct experiments to see how the activation learning works with some disturbed images. Specifically, we add some random lines to the digit images of MNIST for classification, see Fig. 9(c), and investigate the effect of the line width (in pixels) on the classification error rates, see Fig. 9(d). When the width of the randomly added lines is 1, the classification error rate is about 5.7%. It shows that the activation learning can tolerate a certain level of disturbances in images for recognition, even though we haven't taught anything about the disturbances to the



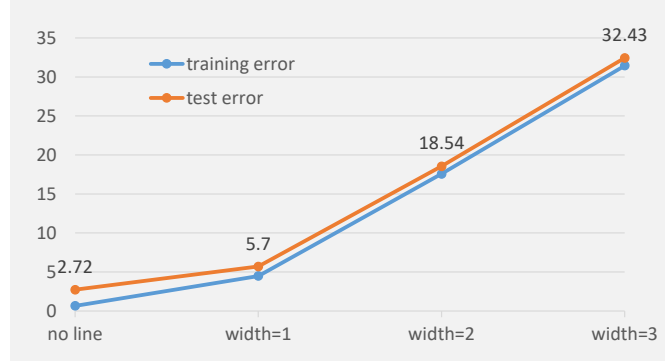
(a) masked



(b) error rates vs. masking ratio



(c) lined



(d) error rates vs. line width

Fig. 9. (a) Masked images with only the top part observable. (b) The classification error rates of the trained two-layer network for masked images of different masking ratios. (c) Images with noisy lines. (d) The classification error rates of the trained two-layer network for randomly-lined images with different line widths.

model. This empowers the activation learning the potential to pass some verification-code systems based on image recognition. When the line width becomes 2, i.e., with stronger disturbances, the error rate increases to 18.5%. With such an error rate, it still has a good chance to successfully pass a verification-code system.

F. Few-Shot Learning

Few-shot learning describes the problem of training a learning model with a very small number of training samples. To study the activation learning as few-shot learning, we create a training set of 10×10 images as shown in Fig. 10(a). In the experiments, we study the case that each digit is trained by n images with $n = 1, 2, 5, 10$, where the training samples are from the first n columns of the 10×10 images, named n -shot learning. To better evaluate the performances we don't use any techniques of data augmentation. Fig. 10(a) gives the test classification accuracies of the activation learning as training progresses. The test accuracy of the 1-shot activation learning is about 48.4%, and with 10 shots, the accuracy increases to about 85.0%. It further confirms the excellence of the activation learning to work with a very small number of training samples. We notice that, expect $n = 1$, the

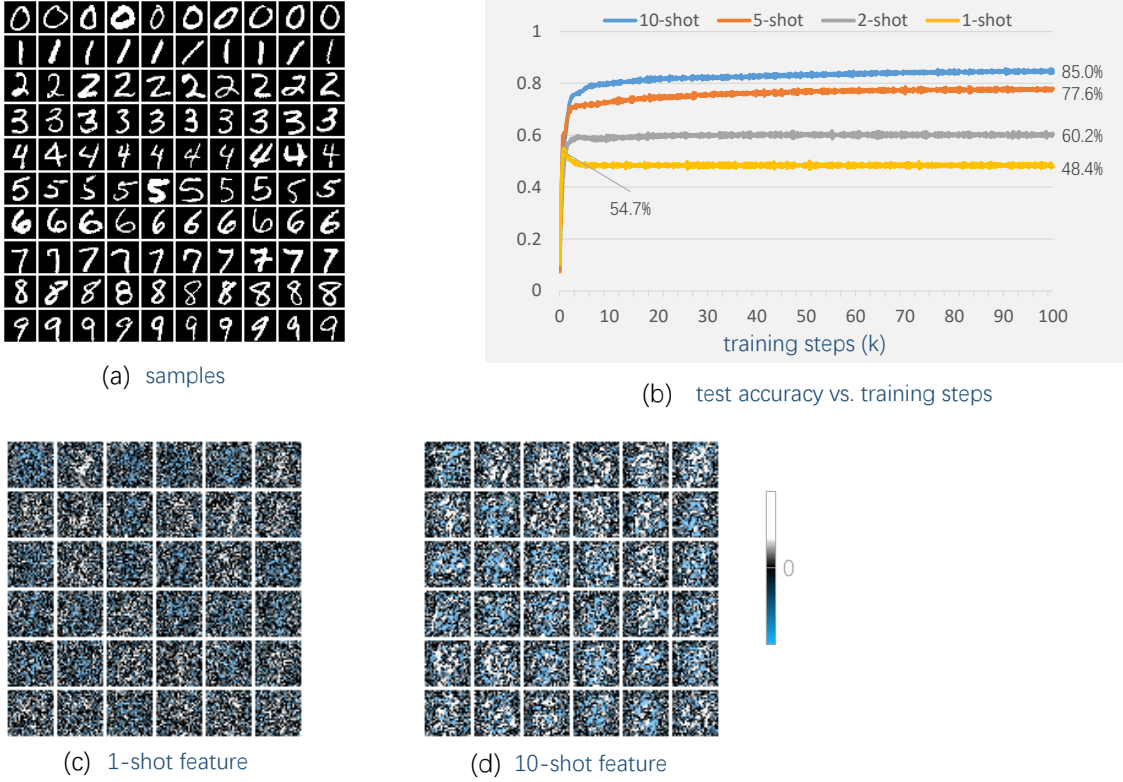


Fig. 10. Few-shot learning. (a) The training samples whose first n columns are used for n -shot learning. (b) The test error rates of the n -shot learning with $n = 1, 2, 5, 10$ as training progresses. (c) The weight patterns of the 36 most activated neurons in the first layer for the 1-shot learning. (d) The weight patterns of the 36 most activated neurons in the first layer for the 10-shot learning.

classification accuracy monotonically increases as training progresses, beyond our expectation. When $n = 1$, the classification accuracy first increases to about 54.7% and then converges to near 48.4%.

We are also interested in the features learned by the few-shot activation learning. According to the asymptotic analysis of the Hebbian learning rule, when $n = 1$, there is a stable solution of the connection weights: 10 of the neurons have weights proportional to the training samples, while the other neurons are deactivated. However, there are infinitely many stable solutions, and it is difficult to reach the one described above. Fig. 10(c) shows the connection weights of the 36 most activated neurons in the first layer with the 1-shot learning, and Fig. 10(d) shows the connection weights with the 10-shot learning. It is observed that the connection weights of the 10-shot learning are enhanced compared to the 1-shot learning.

V. INFERENCE AS GENERATIVE MODELS

Generative models are analog to classification in the framework of activation learning: classification is to infer the categories from the data, and a generative model is opposite - to infer some images or data from nothing or given categories. This section continues working with the previous trained network on MNIST to evaluate several ways of generating digit images.

A. Inference from Partial Information

In activation learning, the inference is conducted to retrieve any missing units (or any subset of the missing units) from the known ones of the input so that the network output activation is maximized. Specifically, let \mathbf{a} be the known units of an input pattern and let \mathbf{z} be the missing units. In the case of image generation, \mathbf{a} is the normalized encoded representation of the given digit, and \mathbf{z} is the image to generate. Let $\mathbf{y}(\mathbf{a}, \mathbf{z})$ be the output activation. The task is to solve an optimization problem:

$$\mathbf{z}^* = \arg \max_{\mathbf{z}} \|\mathbf{y}(\mathbf{a}, \mathbf{z})\|^2 \quad (18)$$

such that $\|\mathbf{z}\| = 1$. We present two methods of solving this problem.

The first method converts the problem to an unconstrained problem and uses the gradient descent method (GD) to find a locally optimal solution:

$$\mathbf{z}^* = \arg \max_{\mathbf{z}} \|\mathbf{y}(\mathbf{a}, \frac{\mathbf{z}}{\|\mathbf{z}\|})\|^2 - (\|\mathbf{z}\|^2 - 1)^2, \quad (19)$$

in which $(\|\mathbf{z}\|^2 - 1)^2$ forces $\|\mathbf{z}\|^2$ to be very close to 1.

The second method is to find a locally optimal solution by iterating $\mathbf{z} \leftarrow \text{norm}(\frac{\partial \|\mathbf{y}\|^2}{\partial \mathbf{z}})$, where $\text{norm}(\cdot) = \frac{(\cdot)}{\|\cdot\|}$ is the normalization operation. This method is derived from the method of Lagrange multipliers, where the Lagrange function is

$$\mathcal{L}(\mathbf{z}) = \|\mathbf{y}(\mathbf{a}, \mathbf{z})\|^2 - \lambda(\|\mathbf{z}\|^2 - 1) \quad (20)$$

and for any optimal solution, its gradient with respect to \mathbf{z} is 0. This leads to $\mathbf{z} = \frac{1}{2\lambda} \frac{\partial \|\mathbf{y}\|^2}{\partial \mathbf{z}}$. Due to the constraint that $\|\mathbf{z}\|^2 - 1 = 0$, it results in $\mathbf{z} = \text{norm}(\frac{\partial \|\mathbf{y}\|^2}{\partial \mathbf{z}})$, leading to the iteration in the method.

B. Image Generation

Given each digit, we use the previous two-layer network trained based on 60000 labeled images to generate some images. In the experiments, for sharpening the generated images, an l_1 -norm term is added to the objective function of (18):

$$\mathbf{z}^* = \arg \max_{\mathbf{z}} \|\mathbf{y}(\mathbf{a}, \mathbf{z})\|^2 - \beta \|\mathbf{z}\|_1 \quad (21)$$

such that $\|\mathbf{z}\| = 1$, where $\beta = 0.003$. Each generated image, starting from a random image in which each pixel is uniformly distributed in $[0, 1/28]$, is optimized with the gradient descent method. Fig. 11(a) shows some randomly generated images, which meet some qualities but lack sufficient diversity, because the generated images are roughly the most probable ones.

To enhance the diversity of the generated images, an idea is to inject some randomness to the network that controls the expressions of some features in the images. In our experiments, we modulate each output of the network by adding some noise so that the resulting output activation is

$$\sum_i (1 + \delta_i) y_i^2$$

where δ_i is a zero-mean Gaussian noise with standard deviation 0.03. This noise affects the contribution of the corresponding features in the generated images. Fig. 11(b) depicts some newly generated images that show improved diversity.

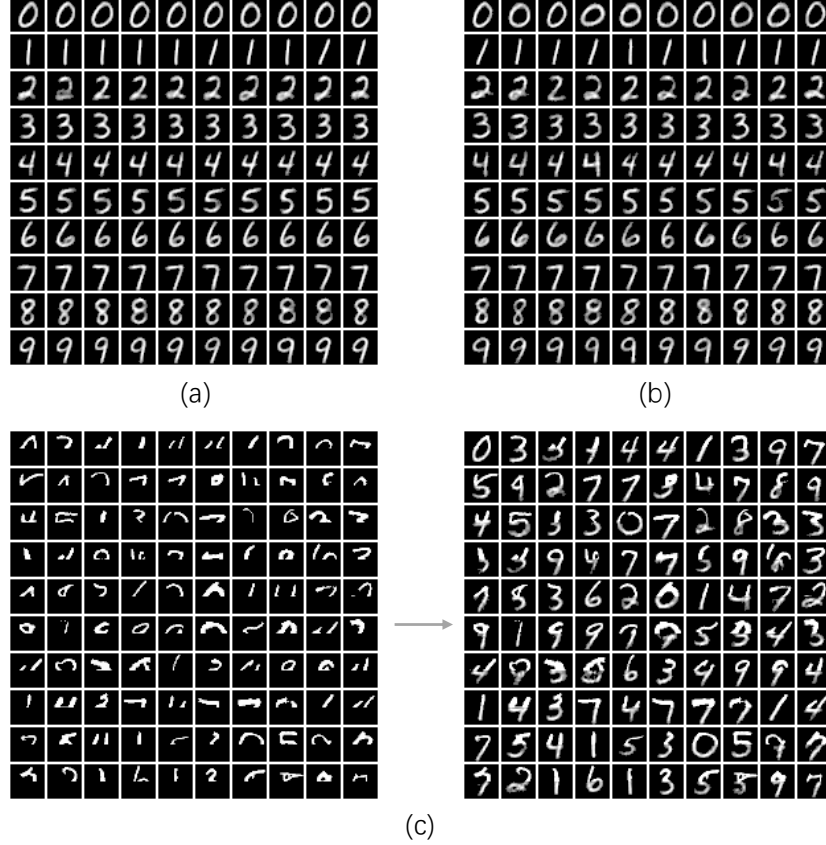


Fig. 11. (a) Generated images without injecting noise. (b) Generated images with injected noise. (c) Masked images and the corresponding completed images.

C. Image Completion

Image completion is another application of the model above. In the experiments, given some masked images from MNIST with only the top half observable, we try to recover the whole images by inference. The task includes two steps - recognizing the digits based on the masked images, and then inferring the missing parts of the images based on the given parts and the predicted digits. The inference is to solve an unconstrained problem:

$$\mathbf{z}_m^* = \arg \max_{\mathbf{z}_m} \|\mathbf{y}(\mathbf{a}, \mathbf{z}_g, \mathbf{z}_m)\|^2, \quad (22)$$

where \mathbf{a} is the normalized encoded representation of the label, \mathbf{z}_g is the given known part of the image, \mathbf{z}_m is the missing part of the image, and $(\mathbf{z}_g, \mathbf{z}_m)$ is jointly normalized before feeding to the network. Fig. 11(c) displays some masked images and the corresponding completed ones. Most of the images are nicely completed, although a small number of completed images look problematic, as there is a certain chance to mis-recognize the digits from only the top half of the images.

VI. NETWORKS WITH LOCAL CONNECTIONS

This section investigates the activation learning on neural networks with local connections, and conducts experiments on CIFAR-10 dataset, which consists of 60000 colour images in 10 categories. Each image has 32×32 pixels. It is demonstrated that local connections without parameter sharing can not only simplify the network complexity but also improve the network performance.

A. Network Model for CIFAR-10

Convolutional networks [2] have been tremendously successful in practical applications of computer vision and time-series processing. Given a convolutional layer, an input pattern is cut into small patches of the same size, which are presented to the same filters for feature detection. The convolution model was originally proposed as a biologically inspired synthesized model. The motivation of convolutional networks is to reduce the number of model parameters and to improve the learning ability of recognizing patterns shifted in location. But it is different from how human brain works, as the parameter sharing mechanism of convolutional layers is not biologically plausible. For the activation learning, we are interested in exploring locally connected layers [50], which have the same structure as the convolutional layers, but without sharing parameters across locations. Fig. 12(a) and (b) compares local connections, in which every local connection has its own weight, with convolutional layers. A locally connected layer has more parameters than a convolutional layer, but in activation learning it allows fewer neurons at each location, and therefore requires less computation. The reason is that in activation learning, all the neurons in a local area compete to represent information, so that the expression ability of each neuron can be effectively utilized. In addition, a locally connected layer can capture some location-related features, which could be useful, for example, when recognizing faces.

Fig. 12(c) is the network model used in our experiments on CIFAR-10. It consists of a few locally connected layers as the hidden layers and one fully connected layer as the output layer. The input of the network is an $32 \times 32 \times 3$ normalized image and an 10×10 encoded label (each category is represented by a row). The square sum of the normalized input images is 2 and that of the encoded label is 1, forcing the model to pay more attention to the structure of the image part. In most of our experiments, we don't apply any data augmentation techniques to focus on the evaluation of the activation learning itself. In the network, each layer has $32 \times 32 \times 3$ units, which are the same size as the input image. For each neuron in a locally connected layer, it connects to the input units in the layer below within a certain distance. Specifically, a neuron located at (i_1, j_1) connects to a neuron at (i_2, j_2) in the layer below if and only if $|i_1 - i_2| \leq K$ and $|j_1 - j_2| \leq K$ for a max range $K \geq 2$. If the neuron is in the first layer, it also connects to all the units of the encoded label. The training of a locally connected layer is the same as training a fully connected layer except it has fewer connections.

The training process on CIFAR-10 is sometimes not stable when taking the absolute function $|\cdot|$ as the activation function. In activation learning, any nonlinear function that does not change the magnitude of the features can serve as a candidate of the activation function. Given any nonlinear function $f(\mathbf{y})$ for a net input \mathbf{y} , we can normalize it

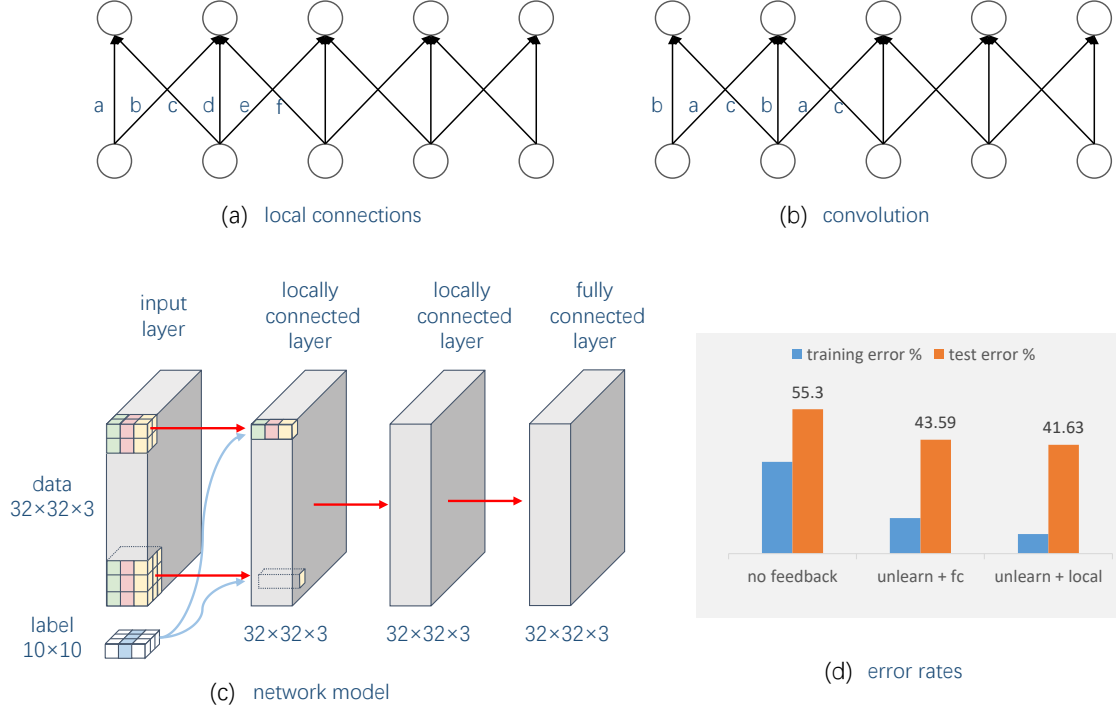


Fig. 12. Activation learning on CIFAR-10. (a) A locally connected layer where each connection has its own weight. (b) A convolutional layer with sharing weight parameters. (c) A network model that consists of a few locally connected layers and one fully connected layer. (d) The error rates of a two-layer network for three cases: fully connected without feedback, fully connected with feedback, and locally connected with feedback.

such that $\|f(\mathbf{y})\|_2 = \|\mathbf{y}\|_2$. The key is to find a nonlinear mapping that preserves most information of the features and makes them easier to represent in a low dimensional space. In our experiments on CIFAR-10, we adopt

$$f(\mathbf{y}) = \beta(|\mathbf{y}| - \overline{|\mathbf{y}|}) \quad (23)$$

as the activation function for a given net input \mathbf{y} . It is simply the zero-mean processing of $|\mathbf{y}|$ by subtracting its mean value, and then re-scaled by a value β such that $\|f(\mathbf{y})\|_2 = \|\mathbf{y}\|_2$.

B. Experiment Results

Fig. 12(d) compares three experiments on CIFAR-10 with a network of two layers (a hidden layer and an output layer). The first experiment studies the performance of the activation learning on a 2-layer fully connected neural network without introducing any feedback, and it achieves about 55.3% error rate. With the help of feedback, this error rate is reduced to about 43.59% in the second experiment, which follows (17) and unlearns negative samples with unlearning factor $\alpha = 1.0$. In the third experiment, we replace the first layer with a locally connected layer of max range $K = 5$, and it leads to an error rate about 41.59%. Local connections in the lower layers help to stabilize learning and improve network performance. A previous benchmark of biologically plausible networks on CIFAR from Krotov and Hopfield reports 49.25% error rate [38], which used a two-layer network of 2000

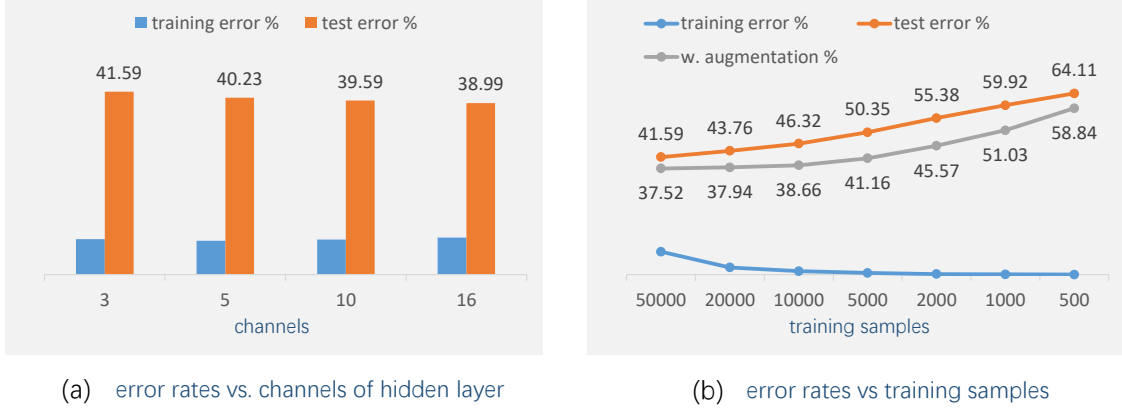


Fig. 13. The error rates of a 2-layer network on CIFAR-10 when the max range of local connections $K = 5$ and the unlearning factor $\alpha = 1.0$. (a) The error rates when the hidden layer has dimension $32 \times 32 \times c$ for different numbers of channels c . (b) The error rates for different numbers of training samples. The orange line is for the case when the hidden layer has dimension $32 \times 32 \times 3$ and no data augmentation is applied. The gray line is for the case when applying data augmentation and the hidden layer has dimension $32 \times 32 \times 16$.

hidden units with the first layer trained in an unsupervised way and the second layer trained by backpropagation. As a comparison, the test error rate of 44.74% is given by the same network trained by pure backpropagation [38]. It is worth emphasizing that the activation learning is completely backpropagation-free, and achieves a better performance.

The performance of the network can be further improved by increasing the width of the network (the number of units in each layer). In the previous experiments, the dimension of the hidden layer is chosen $32 \times 32 \times 3$ with 3 the channel number of the hidden layer. Fig. 13(a) shows that by increasing the channel number of the hidden layer from 3 to 16, the error rate can be reduced to 38.99% from 41.59% when the max range of local connections $K = 5$ and the unlearning factor of feedback $\alpha = 1.0$. Fig. 13(b) continues to study the relationship between the error rates and the sample complexity. The orange line shows that, the error rate increases to about 64.11% from 41.59% when the number of training samples decreases to 500 from 50000. It confirms that the activation learning can work with a relatively small number of training samples. We continue to apply data augmentation to the training samples including randomly cropping the images to the size $28 \times 28 \times 3$, randomly flipping the images horizontally and subtracting off the mean of each image. The gray line in the figure shows the error rates with the data augmentation when the channel number of the hidden layer increases to 16. It introduces a certain performance gain: for 50000 training samples, the error rate decreases to 37.52% from 41.59%, and for 2000 training samples, the error rate decreases to 45.57% from 55.38%.

VII. DISCUSSIONS

Most deep learning models are directional, either discriminative or generative, that transfer inputs patterns to some outputs. For example, the discriminative model takes the data as the input and the label as the supervision of the output, and the generative model is the opposite. This is probably one of the reasons why most of these models

are task-specific, as the networks are prone to extracting features that are only good to construct the outputs and discarding information that might be useful for some other tasks. So, what information should a general-task model learn from data samples? Our answer is that we can learn the statistical distribution of the data samples without distinguishing which part of the samples is the input and which part is the output. Activation learning follows this idea, and its output activation approximately measures how probable an input pattern is, where different parts of the input pattern are bidirectional.

A. Restricted Boltzmann Machines

We briefly compare the activation learning with the Restricted Boltzmann Machines (RBM) [51]. Both are unsupervised learning models that can be used to learn the probability distribution of the training samples. The RBM considers a one-layer network with a visible vector as the input and a hidden binary vector as the output. It assumes that the network assigns every pair of a visible and a hidden vector a probability:

$$p_R(\mathbf{v}, \mathbf{h}) \propto e^{-E(\mathbf{v}, \mathbf{h})}, \quad (24)$$

where $E(\mathbf{v}, \mathbf{h})$ is an energy function depending on the visible vector \mathbf{v} , the hidden vector \mathbf{h} and the connection weights \mathbf{w} . The probability that the network assigns to a variable vector \mathbf{v} is not explicit, which is given by summing over all possible hidden vectors:

$$p_R(\mathbf{v}) \propto \sum_{\mathbf{h}} e^{-E(\mathbf{v}, \mathbf{h})}. \quad (25)$$

This makes both the training and inference of the RBM difficult.

For the activation learning, one can assume that the exponential of the output activation is roughly proportional to the probability of the input vector. Hence, the probability of an input vector \mathbf{v} can be written explicitly as:

$$p_A(\mathbf{v}) \propto e^{\|\mathbf{y}\|^2}, \quad (26)$$

where $\|\mathbf{y}\|^2$ is the network output activation, and $\mathbf{y} = \mathbf{w}^T \mathbf{v}$ for a single layer. Note that the joint probability (24) of the RBM can be rewritten as

$$p_R(\mathbf{v}, \mathbf{h}) \propto e^{\mathbf{h} \cdot \mathbf{y}} \quad (27)$$

if ignoring the bias of the input in the energy function. Comparing (26) with (27) reveals some interesting connections and some differences between the activation learning and the RBM.

B. Variant of the Local Learning Rule

In the local learning rule (4)

$$\Delta w_{ij} = \eta y_j (x_i - \sum_k y_k w_{ik}),$$

the y_j denotes the net input $\sum_u x_u w_{uj}$. With this learning rule, the modification of the connection weights \mathbf{w} is independent of the selection of the nonlinear activation function. This simplifies our analysis of the stable solutions of \mathbf{w} , but in order to work with the activation learning, it requires the nonlinear activation function preserving the magnitude (l_2 norm) of its input. We find that if letting y_i be the output of neuron j instead of being the net

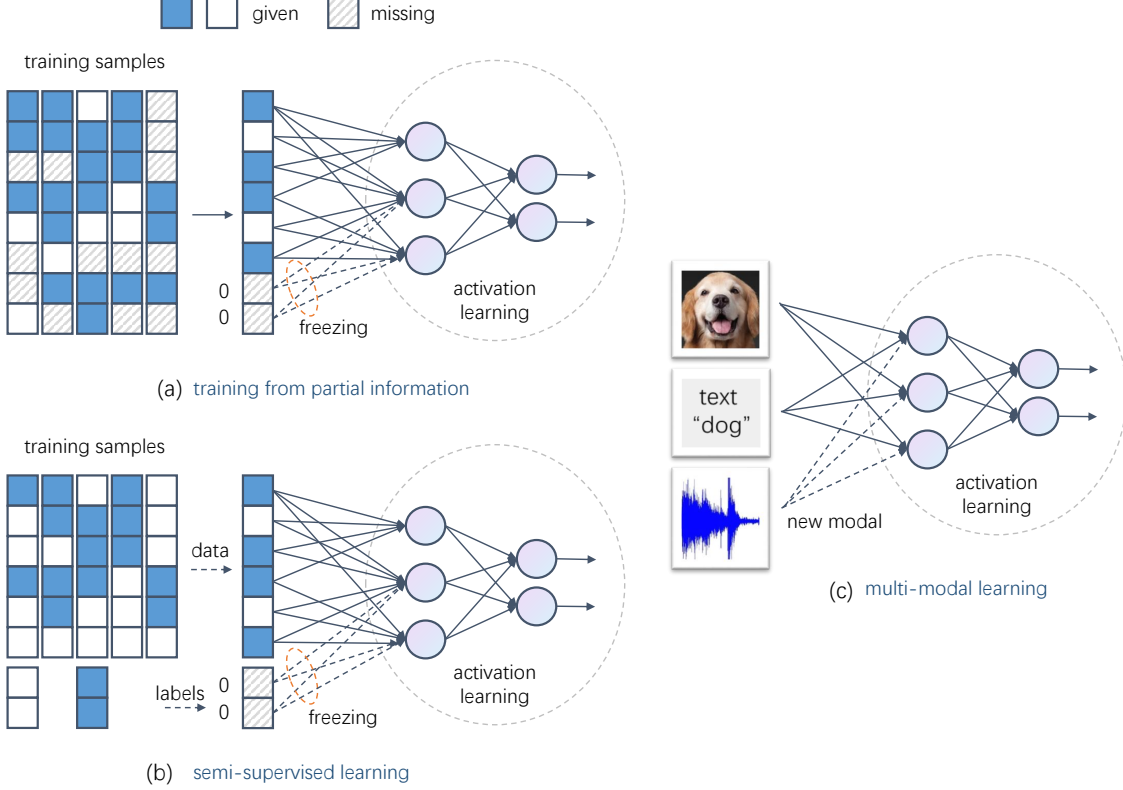


Fig. 14. (a) Activation learning from partial information. (b) Activation learning as semi-supervised learning. (c) Activation learning for multi-modal learning.

input, i.e., $y_i = f(\sum_u x_u w_{uj})$ with a nonlinear activation function f , the learning rule (4) still works. In this case, the nonlinear activation function f does not need to preserve the magnitude of its input, and $\mathbf{w}\mathbf{y} = \mathbf{w}f(\mathbf{w}^T\mathbf{x})$ forms a reconstruction of the input pattern \mathbf{x} . In particular, if using RELU as the activation function, it achieves performance comparable to that presented in previous experiments.

C. Training on Partial Information

There are two key problems about the activation learning that are not well solved in this paper: (1) how to efficiently infer the missing category from any given data for discrimination, and (2) how to efficiently train a network from any partial information. The first problem arises when the number of categories is large, and in this case the brute-force searching method is not efficient any more. Deriving some propagation-style methods for inference that achieve near globally-optimal performances is worth further study.

For the second key problem, it is expected that a network can be trained by giving any subset of the input units at each training step. For example, as demonstrated in Fig. 14(a), given a training sample with some missing units, one may complete the input pattern by filling the missing units with zeros (or other values) and modify the network's connection weights based on the Hebbian learning rule while freezing those connections of the missing units. This makes the activation learning a natural framework of semi-supervised learning, where one can simply

feed either only the data or the data-label pair sample by sample, depending on whether the label is available to the specific sample, as illustrated in Fig. 14(b). It is expected that the unsupervised features (connection weights) learned from unlabeled samples can help the supervised classification tasks, and meanwhile, the supervised label information reshapes the unsupervised features to enhance learning.

D. Associative Memory

This framework of activation learning can also be extended to multi-modal learning when taking multiple modals as the parts of the input, see Fig. 14(c). It is appealing if the network can be trained by any subset of the modals at each time, and build associations among the modals. Such an associative ability, leading to associative memory, is believed to play an essential role in human intelligence [52]. For example, if we provide both the images and texts of some instances to the activation network, it may learn to build the associations between the images and texts. Similarly, if we further provide some sound and text pairs, it may build the associations between sounds and texts. We suspect that statistically related items (which usually appears together) can stimulate activation learning to build their associations as a graph, and the associations can be propagated to create relationship between unrelated items. A further question is how to add new inputs (e.g. new modals) to a well-trained neural network without downgrading its performances on existing tasks. This question, fundamental to supporting multi/general tasks, is difficult to address based on existing deep learning models. But the activation learning looks a promising framework, as the network is simply exploring correlations within input patterns and building associations among different items, potentially paving a road to create multi/general-task neural networks.

VIII. CONCLUSION

This paper developed a biology-inspired local learning rule that raises local competitions within and among neurons, and based on which presented a new learning paradigm named the activation learning. The local learning rule is excellent in discovering local correlations within the input patterns and approximately transforming them to some non-orthogonal principal components. It enables the features in each layer to reconstruct the data in the layer below, thus making the model more resistant to adversarial attack. With this learning rule, one can create a pre-training model to improve the performance of some supervised tasks trained by backpropagation. On the other hand, the activation learning is emerging as a new learning paradigm built on the learning rule, whose output activation approximately measures how probable the input patterns are. This makes activation learning a general framework that unifies supervised learning, unsupervised learning and generative models. Our experiments on MNIST demonstrated that the activation learning can significantly outperform the backpropagation on classification in the low sample-complexity regime, and can generate nice digit images based on the same trained network. It is also robust against some external disturbances such as random masks or noisy lines. With the feedback of accuracy information and the structure of local connections, the performance of the activation learning can be further enhanced, illustrated by experiments on CIFAR. Although there are several key problems to be solved and the performance needs to be further improved, the activation learning is potentially paving a new road to multi/general-task neural networks.

APPENDIX - PROOFS

A. Local Minimum of $E\|\mathbf{x} - \mathbf{w}\mathbf{w}^T\mathbf{x}\|^2$

The mean reconstruction error

$$\|\mathbf{x} - \mathbf{w}\mathbf{w}^T\mathbf{x}\|^2 = \sum_i (x_i - \sum_{j,k} w_{ij}w_{kj}x_k)^2$$

where i, k enumerates the input units and j enumerates the output units.

If we take the partial derivative on the reconstruction error with respect to w_{uv} , it has

$$\begin{aligned} \frac{\partial \|\mathbf{x} - \mathbf{w}\mathbf{w}^T\mathbf{x}\|^2}{\partial w_{uv}} &= -2 \sum_i (x_i - \sum_{j,k} w_{ij}w_{kj}x_k) \left(\left(\sum_k w_{kv}x_k \right) I_{i=u} + w_{iv}x_u \right) \\ &= -2 \left(\sum_k x_u x_k w_{kv} - \sum_{j,k,l} w_{uj}w_{kj}x_k x_l w_{lv} \right) \\ &\quad - 2 \left(\sum_i x_u x_i w_{iv} - \sum_{i,j,k} x_u x_k w_{kj}w_{ij}w_{iv} \right). \end{aligned}$$

It leads to

$$\frac{dE\|\mathbf{x} - \mathbf{w}\mathbf{w}^T\mathbf{x}\|^2}{d\mathbf{w}} = -2[C\mathbf{w} - \mathbf{w}\mathbf{w}^T C\mathbf{w}] - 2[C\mathbf{w} - C\mathbf{w}\mathbf{w}^T\mathbf{w}] \quad (28)$$

with the covariance matrix $C = E\{\mathbf{x}\mathbf{x}^T\}$. We further show that if $C\mathbf{w} - \mathbf{w}\mathbf{w}^T C\mathbf{w} = 0$, then $C\mathbf{w} - C\mathbf{w}\mathbf{w}^T\mathbf{w} = 0$, and as a result the gradient (28) becomes 0. The proof is as follows. If $C\mathbf{w} - \mathbf{w}\mathbf{w}^T C\mathbf{w} = 0$, then $CC\mathbf{w} - C\mathbf{w}\mathbf{w}^T C\mathbf{w} = 0$, and

$$\begin{aligned} CC\mathbf{w} - C\mathbf{w}\mathbf{w}^T C\mathbf{w} &= C(\mathbf{w}\mathbf{w}^T C\mathbf{w}) - C\mathbf{w}\mathbf{w}^T(\mathbf{w}\mathbf{w}^T C\mathbf{w}) \\ &= (C\mathbf{w} - C\mathbf{w}\mathbf{w}^T\mathbf{w})\mathbf{w}^T C\mathbf{w}. \end{aligned}$$

So either $C\mathbf{w} - C\mathbf{w}\mathbf{w}^T\mathbf{w} = 0$ or $\mathbf{w}^T C\mathbf{w} = 0$. If $\mathbf{w}^T C\mathbf{w} = 0$, according to the condition that $C\mathbf{w} - \mathbf{w}\mathbf{w}^T C\mathbf{w} = 0$, $C\mathbf{w} = \mathbf{w}(\mathbf{w}^T C\mathbf{w}) = 0$. This also leads to $C\mathbf{w} - C\mathbf{w}\mathbf{w}^T\mathbf{w} = 0$.

Finally, we get the conclusion that if $C\mathbf{w} - \mathbf{w}\mathbf{w}^T C\mathbf{w} = 0$, then the gradient (28) becomes 0 and such \mathbf{w} is a local minimum point of the mean reconstruction error $\|\mathbf{x} - \mathbf{w}\mathbf{w}^T\mathbf{x}\|^2$.

B. Connection to PCA

We show that the minimum mean square error $E\|\mathbf{x} - \mathbf{w}\mathbf{w}^T\mathbf{x}\|^2$ equals to the reconstruction error of the principal component analysis (PCA). The proof starts from the fact that $\|\mathbf{x} - \mathbf{w}\mathbf{w}^T\mathbf{x}\| \geq \|\mathbf{x} - \mathbf{w}\mathbf{a}_\mathbf{x}\|$ if $\mathbf{a}_\mathbf{x}$ is optimized independently for each \mathbf{x} . The reconstruction error of the PCA equals to the minimized $E\|\mathbf{x} - \mathbf{w}\mathbf{a}_\mathbf{x}\|^2$. This shows that the mean square error $E\|\mathbf{x} - \mathbf{w}\mathbf{w}^T\mathbf{x}\|^2$ cannot be smaller than the reconstruction error of the PCA.

According to the theory of the PCA, $E\|\mathbf{x} - \mathbf{w}\mathbf{a}_\mathbf{x}\|^2$ is minimized if $\mathbf{w} = \mathbf{w}^* = [\mathbf{v}_1, \mathbf{v}_2, \dots, \mathbf{v}_m]$ with \mathbf{v}_j the eigenvector corresponding to the j th largest eigenvalue of the covariance matrix $C = \{\mathbf{x}\mathbf{x}^T\}$ and $\mathbf{a}_\mathbf{x} = \mathbf{w}^{*T}\mathbf{x}$. This leads to the conclusion that the reconstruction error of the PCA equals to $E\|\mathbf{x} - \mathbf{w}^*\mathbf{w}^{*T}\mathbf{x}\|^2$. As a result, the minimum mean square error $E\|\mathbf{x} - \mathbf{w}\mathbf{w}^T\mathbf{x}\|^2$ is not greater than the reconstruction error of the PCA.

Therefore, the minimum mean square error $E\|\mathbf{x} - \mathbf{w}\mathbf{w}^T\mathbf{x}\|^2$ with $m \geq 1$ neurons equals to the reconstruction error of the PCA with m components.

C. Stable Solutions

For any stable solution \mathbf{w} of (8), each column \mathbf{w}_j can be written as a linear combination of $\mathbf{v}_1, \mathbf{v}_2, \dots, \mathbf{v}_m$ with \mathbf{v}_k the eigenvector corresponding to the k th largest eigenvalue of the covariance matrix $C = E\{\mathbf{x}\mathbf{x}^T\}$. The reason is that, for any stable solution \mathbf{w} , it must minimize the reconstruction error $E\|\mathbf{x} - \mathbf{w}\mathbf{w}^T\mathbf{x}\|^2$. According to the discussion in Appendix-B, it must also minimize $E\|\mathbf{x} - \mathbf{w}\mathbf{a}_\mathbf{x}\|^2$ when $\mathbf{a}_\mathbf{x}$ is optimized independently for each \mathbf{x} , which equals to the mean square distance of the samples to the vector space spanned from the columns of \mathbf{w} . Based on the theory of the PCA, in order to minimize this mean square distance, the optimized vector space must be the one spanned from $\mathbf{v}_1, \mathbf{v}_2, \dots, \mathbf{v}_m$ with \mathbf{v}_j the eigenvector corresponding to the j th largest eigenvalue λ_i of the covariance matrix $C = \{\mathbf{x}\mathbf{x}^T\}$. As a consequence, each column of a stable \mathbf{w} must be a linear combination of $\mathbf{v}_1, \mathbf{v}_2, \dots, \mathbf{v}_m$.

When the number of neurons $m = 2$, let a solution $\mathbf{w} = [\mathbf{w}_1, \mathbf{w}_2]$ be

$$\mathbf{w}_1 = u_{11}\mathbf{v}_1 + u_{12}\mathbf{v}_2,$$

$$\mathbf{w}_2 = u_{21}\mathbf{v}_1 + u_{22}\mathbf{v}_2.$$

We show that the solution \mathbf{w} is stable if and only if $u_{11}^2 + u_{21}^2 = 1$ and $u_{12}^2 + u_{22}^2 = 1$. The argument can be naturally extended to a general m .

If \mathbf{w} is stable, then $C\mathbf{w} = \mathbf{w}\mathbf{w}^T C\mathbf{w}$, where

$$C\mathbf{w} = [\lambda_1 u_{11}\mathbf{v}_1 + \lambda_2 u_{12}\mathbf{v}_2, \lambda_1 u_{21}\mathbf{v}_1 + \lambda_2 u_{22}\mathbf{v}_2], \quad (29)$$

$$\begin{aligned} \mathbf{w}\mathbf{w}^T C\mathbf{w} &= ((u_{11}^2 + u_{21}^2)\mathbf{v}_1\mathbf{v}_1^T + (u_{12}^2 + u_{22}^2)\mathbf{v}_2\mathbf{v}_2^T)C\mathbf{w} \\ &= [(u_{11}^2 + u_{21}^2)\lambda_1 u_{11}\mathbf{v}_1 + (u_{12}^2 + u_{22}^2)\lambda_2 u_{12}\mathbf{v}_2, \lambda_1 u_{21}\mathbf{v}_1 + \lambda_2 u_{22}\mathbf{v}_2]. \end{aligned} \quad (30)$$

From which, we can get that $u_{11}^2 + u_{21}^2 = 1$ and $u_{12}^2 + u_{22}^2 = 1$. Inversely, if $u_{11}^2 + u_{21}^2 = 1$ and $u_{12}^2 + u_{22}^2 = 1$, we can also get that $C\mathbf{w} = \mathbf{w}\mathbf{w}^T C\mathbf{w}$ from the above equations. In this case, \mathbf{w} is stable, reaching the above conclusion. This result also tells us that there are infinitely many stable solutions when $m > 1$.

Based on this result, we can also get that for a stable solution \mathbf{w} with $m = 2$,

$$\|\mathbf{w}\|^2 = \sum_{ij} w_{ij}^2 = \mathbf{w}_1^T \mathbf{w}_1 + \mathbf{w}_2^T \mathbf{w}_2 = u_{11}^2 + u_{21}^2 + u_{12}^2 + u_{22}^2 = 2.$$

Extending the proof to a general m yields

$$\|\mathbf{w}\|^2 = m. \quad (31)$$

D. Activation Bound

We show that with the learning rule (4), $\|\mathbf{y}\|^2 = \|\mathbf{w}^T \mathbf{x}\|^2$ tends to be upper bounded by $\|\mathbf{x}\|^2$. Let \mathbf{w}_j be the j th column of \mathbf{w} , from (7), it derives

$$\begin{aligned} \Delta(y_j^2) &= \Delta(\mathbf{w}_j^T \mathbf{x})^2 \\ &= 2\eta \mathbf{w}_j^T \mathbf{x} \mathbf{x}^T (\mathbf{x} \mathbf{x}^T \mathbf{w}_j - \mathbf{w}(\mathbf{w}^T \mathbf{x} \mathbf{x}^T \mathbf{w}_j)) + O(\eta^2) \\ &= 2\eta [\mathbf{w}_j^T \mathbf{x} \mathbf{x}^T \mathbf{x} \mathbf{x}^T \mathbf{w}_j - \sum_k (\mathbf{w}_k^T \mathbf{x} \mathbf{x}^T \mathbf{w}_j)^2] + O(\eta^2) \\ &\leq 2\eta [(\mathbf{w}_j^T \mathbf{x})^2 \|\mathbf{x}\|^2 - (\mathbf{w}_j^T \mathbf{x})^2 (\sum_k (\mathbf{w}_k^T \mathbf{x})^2)] + O(\eta^2) \\ &= 2\eta y_j^2 (\|\mathbf{x}\|^2 - \|\mathbf{y}\|^2) + O(\eta^2). \end{aligned}$$

As long as $\|\mathbf{y}\|^2$ is larger than $\|\mathbf{x}\|^2$, $\Delta(y_j^2)$ is smaller than 0 if the learning rate η is sufficiently small, driving $|y_j|$ to be smaller. As a result, $\|\mathbf{y}\|^2$ tends to be upper bounded by $\|\mathbf{x}\|^2$.

E. Activation as Typicality

We show that the total amount of the output activation $\|\mathbf{y}\|^2$ tends to be upper bounded by $\|\mathbf{x}\|^2 - d^2(\mathbf{x}, V)$ when the output dimension m is smaller than the input dimension, where $d(\mathbf{x}, V)$ is the distance from \mathbf{x} to the linear space V spanned from the eigenvectors $\mathbf{v}_1, \mathbf{v}_2, \dots, \mathbf{v}_m$ corresponding to the m largest eigenvalues of the covariance matrix $C = \{\mathbf{x} \mathbf{x}^T\}$.

The idea is to construct a new input \mathbf{x}' , which is the projection of \mathbf{x} to the linear space V . It is

$$\mathbf{x}' = \sum_{k=1}^m (\mathbf{x}^T \mathbf{v}_k) \mathbf{v}_k.$$

It is easy to verify that when taking \mathbf{x}' as the input instead of \mathbf{x} , the net input is still \mathbf{y} . According to our result on the bound of the output activation, $\|\mathbf{y}\|^2$ tends to be bounded by

$$\|\mathbf{x}'\|^2 = \sum_{k=1}^m (\mathbf{x}^T \mathbf{v}_k)^2 = \|\mathbf{x}\|^2 - d^2(\mathbf{x}, V).$$

REFERENCES

- [1] D. E. Rumelhart, G. E. Hinton, and R. J. Williams, "Learning representations by back-propagating errors," *nature*, vol. 323, no. 6088, pp. 533–536, 1986.
- [2] A. Krizhevsky, I. Sutskever, and G. E. Hinton, "Imagenet classification with deep convolutional neural networks," *Communications of the ACM*, vol. 60, no. 6, pp. 84–90, 2017.
- [3] K. He, X. Zhang, S. Ren, and J. Sun, "Deep residual learning for image recognition," in *Proceedings of the IEEE conference on computer vision and pattern recognition*, 2016, pp. 770–778.
- [4] J. Devlin, M.-W. Chang, K. Lee, and K. Toutanova, "Bert: Pre-training of deep bidirectional transformers for language understanding," *arXiv preprint arXiv:1810.04805*, 2018.
- [5] I. Goodfellow, J. Pouget-Abadie, M. Mirza, B. Xu, D. Warde-Farley, S. Ozair, A. Courville, and Y. Bengio, "Generative adversarial networks," *Communications of the ACM*, vol. 63, no. 11, pp. 139–144, 2020.
- [6] D. Silver, A. Huang, C. J. Maddison, A. Guez, L. Sifre, G. Van Den Driessche, J. Schrittwieser, I. Antonoglou, V. Panneershelvam, M. Lanctot *et al.*, "Mastering the game of go with deep neural networks and tree search," *nature*, vol. 529, no. 7587, pp. 484–489, 2016.

- [7] D. Silver, J. Schrittwieser, K. Simonyan, I. Antonoglou, A. Huang, A. Guez, T. Hubert, L. Baker, M. Lai, A. Bolton *et al.*, “Mastering the game of go without human knowledge,” *nature*, vol. 550, no. 7676, pp. 354–359, 2017.
- [8] M. Moravčík, M. Schmid, N. Burch, V. Lisý, D. Morrill, N. Bard, T. Davis, K. Waugh, M. Johanson, and M. Bowling, “Deepstack: Expert-level artificial intelligence in heads-up no-limit poker,” *Science*, vol. 356, no. 6337, pp. 508–513, 2017.
- [9] F. Crick, “The recent excitement about neural networks,” *Nature*, vol. 337, no. 6203, pp. 129–132, 1989.
- [10] J. L. McClelland, “How far can you go with hebbian learning, and when does it lead you astray,” *Processes of change in brain and cognitive development: Attention and performance xxi*, vol. 21, pp. 33–69, 2006.
- [11] A. H. Marblestone, G. Wayne, and K. P. Kording, “Toward an integration of deep learning and neuroscience,” *Frontiers in computational neuroscience*, p. 94, 2016.
- [12] J. C. Whittington and R. Bogacz, “Theories of error back-propagation in the brain,” *Trends in cognitive sciences*, vol. 23, no. 3, pp. 235–250, 2019.
- [13] S. Grossberg, “Competitive learning: From interactive activation to adaptive resonance,” *Cognitive science*, vol. 11, no. 1, pp. 23–63, 1987.
- [14] B. D. McCandliss, J. A. Fiez, A. Protopapas, M. Conway, and J. L. McClelland, “Success and failure in teaching the [r]-[l] contrast to japanese adults: Tests of a hebbian model of plasticity and stabilization in spoken language perception,” *Cognitive, Affective, & Behavioral Neuroscience*, vol. 2, no. 2, pp. 89–108, 2002.
- [15] M. F. Bear and R. C. Malenka, “Synaptic plasticity: Ltp and ltd,” *Current opinion in neurobiology*, vol. 4, no. 3, pp. 389–399, 1994.
- [16] D. E. Rumelhart and D. Zipser, “Feature discovery by competitive learning,” *Cognitive science*, vol. 9, no. 1, pp. 75–112, 1985.
- [17] R. Guillery, “Binocular competition in the control of geniculate cell growth,” *Journal of Comparative Neurology*, vol. 144, no. 1, pp. 117–129, 1972.
- [18] K. D. Miller, “Synaptic economics: competition and cooperation in synaptic plasticity,” *Neuron*, vol. 17, no. 3, pp. 371–374, 1996.
- [19] J. P. Bourgeois, P. J. Jastreboff, and P. Rakic, “Synaptogenesis in visual cortex of normal and preterm monkeys: evidence for intrinsic regulation of synaptic overproduction,” *Proceedings of the National Academy of Sciences*, vol. 86, no. 11, pp. 4297–4301, 1989.
- [20] S. Pallas and B. Finlay, “Compensation for population size mismatches in the hamster retinotectal system: alterations in the organization of retinal projections,” *Visual neuroscience*, vol. 6, no. 3, pp. 271–281, 1991.
- [21] K. D. Miller and D. J. MacKay, “The role of constraints in hebbian learning,” *Neural computation*, vol. 6, no. 1, pp. 100–126, 1994.
- [22] S. Song, K. D. Miller, and L. F. Abbott, “Competitive hebbian learning through spike-timing-dependent synaptic plasticity,” *Nature neuroscience*, vol. 3, no. 9, pp. 919–926, 2000.
- [23] G. G. Turrigiano, K. R. Leslie, N. S. Desai, L. C. Rutherford, and S. B. Nelson, “Activity-dependent scaling of quantal amplitude in neocortical neurons,” *Nature*, vol. 391, no. 6670, pp. 892–896, 1998.
- [24] G. W. Davis and C. S. Goodman, “Synapse-specific control of synaptic efficacy at the terminals of a single neuron,” *Nature*, vol. 392, no. 6671, pp. 82–86, 1998.
- [25] E. L. Bienenstock, L. N. Cooper, and P. W. Munro, “Theory for the development of neuron selectivity: orientation specificity and binocular interaction in visual cortex,” *Journal of Neuroscience*, vol. 2, no. 1, pp. 32–48, 1982.
- [26] J. S. Isaacson and M. Scanziani, “How inhibition shapes cortical activity,” *Neuron*, vol. 72, no. 2, pp. 231–243, 2011.
- [27] H. Markram, M. Toledo-Rodriguez, Y. Wang, A. Gupta, G. Silberberg, and C. Wu, “Interneurons of the neocortical inhibitory system,” *Nature reviews neuroscience*, vol. 5, no. 10, pp. 793–807, 2004.
- [28] D. L. Meinecke and A. Peters, “Gaba immunoreactive neurons in rat visual cortex,” *Journal of Comparative Neurology*, vol. 261, no. 3, pp. 388–404, 1987.
- [29] F. Rosenblatt, “Principles of neurodynamics. perceptrons and the theory of brain mechanisms,” Cornell Aeronautical Lab Inc Buffalo NY, Tech. Rep., 1961.
- [30] C. Von der Malsburg, “Self-organization of orientation sensitive cells in the striate cortex,” *Kybernetik*, vol. 14, no. 2, pp. 85–100, 1973.
- [31] S. Grossberg, “Adaptive pattern classification and universal recoding: I. parallel development and coding of neural feature detectors,” *Biological cybernetics*, vol. 23, no. 3, pp. 121–134, 1976.
- [32] K. Fukushima, “Cognitron: A self-organizing multilayered neural network,” *Biological cybernetics*, vol. 20, no. 3, pp. 121–136, 1975.
- [33] T. Kohonen, “Self-organized formation of topologically correct feature maps,” *Biological cybernetics*, vol. 43, no. 1, pp. 59–69, 1982.
- [34] R. Linsker, “From basic network principles to neural architecture: emergence of spatial-opponent cells,” *Proceedings of the National Academy of Sciences*, vol. 83, no. 19, pp. 7508–7512, 1986.
- [35] G. J. Goodhill, “Topography and ocular dominance: a model exploring positive correlations,” *Biological cybernetics*, vol. 69, no. 2, pp. 109–118, 1993.

- [36] T. Shinozaki, “Biologically inspired feedforward supervised learning for deep self-organizing map networks,” *MLINI Workshop in NIPS*, 2016.
- [37] A. Makhzani and B. Frey, “A winner-take-all method for training sparse convolutional autoencoders,” in *NIPS Deep Learning Workshop*. Citeseer, 2014.
- [38] D. Krotov and J. J. Hopfield, “Unsupervised learning by competing hidden units,” *Proceedings of the National Academy of Sciences*, vol. 116, no. 16, pp. 7723–7731, 2019.
- [39] L. Grinberg, J. Hopfield, and D. Krotov, “Local unsupervised learning for image analysis,” *arXiv preprint arXiv:1908.08993*, 2019.
- [40] T. Shinozaki, “Biologically-motivated deep learning method using hierarchical competitive learning,” *arXiv preprint arXiv:2001.01121*, 2020.
- [41] N. B. Ravichandran, A. Lansner, and P. Herman, “Brain-like approaches to unsupervised learning of hidden representations-a comparative study,” in *International Conference on Artificial Neural Networks*. Springer, 2021, pp. 162–173.
- [42] M. Gupta, A. Ambikapathi, and S. Ramasamy, “Hebbnet: A simplified hebbian learning framework to do biologically plausible learning,” in *ICASSP 2021-2021 IEEE International Conference on Acoustics, Speech and Signal Processing (ICASSP)*. IEEE, 2021, pp. 3115–3119.
- [43] S.-L. Huang, X. Xu, L. Zheng, and G. W. Wornell, “An information theoretic interpretation to deep neural networks,” in *2019 IEEE international symposium on information theory (ISIT)*. IEEE, 2019, pp. 1984–1988.
- [44] E. Oja, “Simplified neuron model as a principal component analyzer,” *Journal of mathematical biology*, vol. 15, no. 3, pp. 267–273, 1982.
- [45] Y. Qin, N. Frosst, S. Sabour, C. Raffel, G. Cottrell, and G. Hinton, “Detecting and diagnosing adversarial images with class-conditional capsule reconstructions,” *arXiv preprint arXiv:1907.02957*, 2019.
- [46] R. A. Nawrocki, R. M. Voyles, and S. E. Shaheen, “A mini review of neuromorphic architectures and implementations,” *IEEE Transactions on Electron Devices*, vol. 63, no. 10, pp. 3819–3829, 2016.
- [47] T.-H. Chan, K. Jia, S. Gao, J. Lu, Z. Zeng, and Y. Ma, “Pcanet: A simple deep learning baseline for image classification?” *IEEE transactions on image processing*, vol. 24, no. 12, pp. 5017–5032, 2015.
- [48] L. Zaadnoordijk, T. R. Besold, and R. Cusack, “Lessons from infant learning for unsupervised machine learning,” *Nature Machine Intelligence*, vol. 4, no. 6, pp. 510–520, 2022.
- [49] P. Simard, Y. LeCun, and J. Denker, “Efficient pattern recognition using a new transformation distance,” *Advances in neural information processing systems*, vol. 5, 1992.
- [50] Y. L. Cun, “Learning process in an asymmetric threshold network,” in *Disordered systems and biological organization*. Springer, 1986, pp. 233–240.
- [51] G. Hinton, “A practical guide to training restricted boltzmann machines,” *Momentum*, vol. 9, no. 1, pp. 926–947, 2010.
- [52] J. R. Anderson and G. H. Bower, *Human associative memory*. Psychology press, 2014.